Developments in ICP-MS: electrochemically modulated liquid chromatography for the clean-up of ICP-MS blanks and reduction of matrix effects by flow injection ICP-MS

By

Cory Thomas Gross

A dissertation submitted to the graduate faculty

in partial fulfillment of the requirements for the degree of

DOCTOR OF PHILOSOPHY

Major: Analytical Chemistry

Program of Study Committee:
R.S. Houk, Major Professor
Patricia Thiel
David Laird
Mei Hong
Hans Stauffer

Iowa State University

Ames, Iowa

2008

TABLE OF CONTENTS

Abstract

The focus of this dissertation is the development of techniques with which to enhance the existing abilities of inductively coupled plasma mass spectrometry (ICP-MS). ICP-MS is a powerful technique for trace metal analysis in samples of many types, but like any technique it has certain strengths and weaknesses. Attempts are made to improve upon those strengths and to overcome certain weaknesses.

One standout figure of merit for ICP-MS is limit of detection. With today's advances in instrumental hardware the limit of detection is often limited by the purity of the blank. While the limit of detection itself is not evaluated, by improving blank cleanliness it is theoretically possible to get improvements in this area. A metal-free, low-pressure, electrochemically modulated liquid chromatography (EMLC) column was designed and evaluated specifically for use on-line with ICP-MS. The EMLC column reduces levels of trace elements in blank solutions just before the blank is introduced into the nebulizer. The stationary phase is reticulated vitreous carbon (RVC), and the reference and counter electrodes are positioned upstream from the column to minimize contamination. Many metal ions can be removed at a single applied potential of ~-0.75 V (vs SHE).

Analysis of samples with high matrix concentrations is a relative area of weakness for ICP-MS. Solution samples with matrix concentrations above ~0.1% generally present difficulties due to cone clogging and matrix effects. Flow injection (FI) is coupled to ICP-MS to reduce clogging from samples such as 1% sodium salts and seawater. Surprisingly, matrix effects are also less severe during flow injection, at least for some matrix elements on

the particular instrument used. Sodium chloride at 1% Na and undiluted seawater cause only 2 to 29 % losses of signal for typical analyte elements. A heavy matrix element (Bi) at 0.1% also induces only ~14% loss of analyte signal. However, barium causes about the same matrix effect as usual. Also, matrix effects during FI are of the usual magnitude when a metal shield is inserted between the load coil and torch, which is the most common mode of operation for the particular ICP-MS device used.

Chapter 1. General Introduction

Historical Perspective

The history of inductively coupled plasma (ICP) as an analytical tool began in the 1960s. Greenfield [1] and Wendt and Fassel [2] independently began working on harnessing the ICP as an excitation source for trace metal analysis. Their work led to ICP- atomic emission spectroscopy (AES) being one of the most powerful analytical atomic spectroscopy tools of the 1970s.

Inductively coupled plasma mass spectrometry (ICP-MS) grew out of experiments in 1974 by Gray [3,4], who used a DC arc plasma in conjunction with a mass spectrometer for sensitive elemental analysis. The full potential of ICP-MS was harnessed in 1980 when Houk et al. [5] developed a high temperature plasma source capable of a wide array of elemental speciation.

The modern ICP-MS instrument is capable of multi-element analysis which is extremely sensitive and has high selectivity. Detection limits of parts per trillion are routine and parts per quadrillion are obtainable. The linear dynamic range is larger than that of many analytical tools at 8 orders of magnitude [6].

While the field of atomic spectroscopy and ICP-MS may seem mature, new developments and applications are still occurring rapidly.

Fundamental Aspects of ICP-MS

An inductively coupled plasma (ICP) is an atmospheric pressure electrical discharge ionization source. The plasma is formed when argon gas is passed through three concentric quartz tubes otherwise known as a Fassel plasma torch (figure 1). The outer tube carries the bulk of the argon (~15 L/min) known as the outer gas. The intermediate tube carrying the auxiliary gas (~1 l/min) sheathes the injector tube and prevents it from melting when the plasma is started. The inner tube carries the sample gas (~1 L/min) which carries the aerosol sample. The end of the torch is surrounded by a coil of water cooled copper tubing known as the load coil. The load coil is supplied with 800-2000 W of power from an RF generator providing high frequency current at typically 40.68 or 27.12 MHz. The plasma is then ignited by seed electrons from a Tesla coil. These seed electrons interact with the magnetic field of the load coil causing electrons of high kinetic energy. When these electrons collide with Ar atoms, Ar^+ ions are produced along with more electrons. This cycle continues until a stable, high temperature plasma is produced.

The resultant plasma is “doughnut” shaped with a highly energetic induction region surrounding the central channel. The central channel is punched through the induction region by the sample gas and provides an efficient path for sample aerosol to pass through. The temperature of the central channel of the plasma is ~7000K, which is cooler than the ~10,000K induction region , but is still sufficient for ionization. As the sample aerosol passes thought the central channel it is desolvated, vaporized, atomized, and ionized for analysis by mass spectrometry (figure 2). The central channel itself has two zones, the initial radiation zone (IRZ) and the normal analytical zone (NAZ). The positively charged sample

ions are the most concentrated in the beginning of the NAZ and this is generally where the mass spectrometer interface is positioned (figure 3).

At the interface of the mass spectrometer the ion beam must be extracted. This is achieved by placing a sampling cone with a small orifice (~1.1 mm) in the NAZ of the plasma. The ion beam then enters an interface region pumped down to a pressure of ~ 1 torr and passes through a skimmer cone with a smaller orifice than the sampler (1 – 0.4 mm). At this point the ion beam reaches the mass spectrometer.

ICP-MS Instrumentation

The experiments described in this dissertation were all performed on an HP 4500 series (now Agilent, Santa Clara, CA) ICP-MS (figure 4). The HP 4500 is a bench top ICP-MS with a single quadrupole mass analyzer and is considered a low resolution (R=~400) instrument. This resolution is generally sufficient for the resolving power of 1 amu required by these experiments.

Two different nebulizers were employed in the experiments; a Babington and a PFA microconcentric. The Babington nebulizer (figure 5) is a robust nebulizer that works at relatively higher flow rates and provides less sensitivity. It consists of a vertical groove with two holes, one positioned above the other. As the sample solution is pumped out of the top hole it flows down to the bottom hole through which a stream of Ar is passed causing nebulization. The 100 µl/min PFA microconcentric nebulizer (ESI, Omaha, NE) (figure 6) provides more sensitivity and lower sample uptake, but can become clogged (stalling uptake)

more easily. The microconcentric nebulizer consists an inner tube which carries solution to the tip where it is nebulized by the outer sheath of Ar gas.

A double-pass Scott type spray chamber (figure 7) was used in these experiments. The spray chamber acts as a droplet size filter and allows only sample droplets below an appropriate size from the nebulizer to enter the plasma. The spray chamber was operated at 2°C to condense water vapor more efficiently and reduce the solvent load on the plasma.

After the sample has passed through the plasma and the ion beam reaches the mass spectrometer, photons and neutral species need to be removed. This is achieved by deflecting the ion beam off-axis via the Omega lenses (figure 8). The ion beam now enters the quadrupole mass analyzer (figure 9), the most common type of mass analyzer in ICP-MS. Ions are separated based on their mass to charge ratio (m/z) by a combination of DC and AC electrical fields.

Blank Purity in ICP-MS

Current ICP-MS instrumentation has reached a point in its development in which many requirements for improved detection limits have been satisfied. Magnetic sector mass analyzers, in particular, can routinely reach limits of detection in the parts per trillion regime for various elements. In some cases though, this theoretical detection limit cannot be reached in practice due to impure blank solutions. Thus in reality the detection limit is often limited by the cleanliness of the blank resulting in a waste of some of the analysis power of an expensive instrument.

The importance of pure blanks when performing ultra trace analysis cannot be overstated, and experimentalists often go to great lengths to get them. Laboratories invest time and money in clean rooms, very expensive ultra clean acids, extensive acid washing of containers, and sub-boiling distillation rigs. Obviously cost becomes a factor as clean rooms may be too expensive. Ultra pure acids can cost $600 per L [7] and unless they are opened in a very clean environment can become contaminated quite quickly.

Sub-boiling distillation (figure 10) is a popular way to produce clean acid in-house. This process involves gently heating the "dirty" acid to a temperature under the boiling point but high enough induce some acid vaporization, leaving contaminants in the bulk liquid. These acid vapors are collected in the cooled "clean" side of the apparatus. Sub-boiling distillation for this purpose has been discussed by Keuhner et al. [8]. It can be a very effective technique, but has some drawbacks. It is generally quite slow as it can take a day to produce 100 ml of clean acid with a basic setup. The sub-boiling process is also less effective at the removal of some contaminant elements with low boiling points, such as As and Hg. These types of elements vaporize at a sufficiently low temperature to be transferred with the clean acid. A similar problem occurs when trying to purify acids with high boiling points such as sulfuric acid. In this case the acid must be raised to a relatively high temperature to be vaporized and many contaminants of intermediate boiling point are again carried over with the clean acid vapor.

Storage of clean acids can also be problematic. Over time the acid can leach certain elements from the container resulting in degradation of purity [9]. Thus an on-line means of purification may be the best possible way to achieve low blank signals.

Previous EMLC Experiments

The feasibility of the use of electrochemically modulated liquid chromatography to clean up ICP-MS blanks has been studied by Hasan and Houk et al [10]. The EMLC column was of a design by Porter et al [11]. It was primarily used as a liquid chromatography technique used to separate various organic compounds such as aromatic sulfates [12], separation of inorganic anions [13], and in electrospray mass spectrometry [14].

A detailed description of this column is found elsewhere [11]. A basic blueprint of the column is shown here (figure 11). A tube of Nafion® ion exchange membrane is inserted into a porous stainless steel tube (pore size ~2µm) and the ends of the membrane are flanged to hold it in place. A porous stainless steel frit is secured to one end at which time the column can be slurry packed with porous graphitic carbon (PGC) spheres of ~7µm diameter. The PGC is suspended in a 50:50 acetonitrile: dibromomethane mixture at 8000 psi. The other end of the column is then capped with a PEEK-alloyed Teflon (PAT) frit.

The column is then treated as a three electrode chemical cell. The stainless steel housing acts as the counter electrode and the PGC packing serves as the working electrode. A Ag/AgCl (sat'd NaCl) reference electrode is outside of the column in a glass electrolyte reservoir surrounding the column. This reservoir is filled with supporting electrolyte, in this case 0.1% nitric acid.

This column demonstrated the successful removal of several contaminant elements, many at 99% efficiency or better. Cd, Cu, Ag, V, Co, Zn, Cr, Pb, Sn and Tl were shown to

be removal candidates from 0.1% nitric and/or D.I. water. Another valuable discovery was the ability to retain U, an important element in semiconductor materials as its radioactive decay ruins the band gap.

While proof of concept was gained through these experiments several parts of the column were not ideal for the purpose of cleaning ICP-MS blanks. Probably the most obvious was the use of stainless steel parts in the housing and frit. Stainless steel contains some of the elements it would be desirable to remove. The acids in this experiment were of low enough concentration to not cause much leaching of these elements, but ICP-MS blanks are often of acid concentrations of 1% or greater which were found to damage the column. Also the nature of the high pressure packing of uniform PGC necessary for traditional LC separation makes a high pressure pump necessary. For the purposes of ICP-MS this results in a larger degree of pump noise which is undesirable in detection limit measurements. The ion exchange membrane also presents a challenge as it is not very robust. Some metal contaminants may require more negative potentials for removal than can be feasibly obtained in this column. At applied potentials more negative than -0.55 V vs. Ag/AgCl H_2 (g) evolves from 0.1% nitric acid causing the membrane to rupture and a failure in functionality of the column.

Matrix Effects in ICP-MS

Matrix effects are the general term given to changes in analyte sensitivity caused by variable concentrations of matrix elements [15]. Generally, increasing the concentration of matrix elements in the plasma results in a reduction of the sensitivity for analyte ions [16-24], in a few cases the matrix actually increasing sensitivity [25]. Besides matrix concentration,

the matrix and analyte atomic weights also play a role in the severity of matrix effects. The greatest effects are generally seen when the analyte is of low mass and the matrix is of heavy mass. Because of these matrix effects the total solute levels in ICP-MS are usually kept to less than 0.1% in practical applications. Even when this rule of thumb is obeyed, correction techniques such as internal standardization, isotope dilution, or standard additions are often necessary [6, 26,27].

A review by Niu and Houk [15] discusses how matrix effects are often attributed to space charge effects. The maximum current (I_{max}) that an ion lens can transmit is given by the equation:

$$I_{max/}\,\mu A = 0.9\,(z/m)^{1/2}(D/L)^2V^{3/2} \qquad (1)$$

Where

z/m = charge to mass ratio of the major background ion (1/40 for Ar^+)

D = diameter of ion lens

L = length of ion lens

V = kinetic energy of major background ions (~ 5 eV)

For the ICP-MS interface I_{max}~ 0.4 μA and the actual ion current through a typical skimmer ~1.5 mA. Thus according to Eq. 1 severe space charge effects can be expected behind the skimmer [16,28-31].

When an ion passes through the skimmer and enters the ion lens the trajectory of that ion is dependent on changes in the composition of the ion beam, including ions from the matrix element. According to space charge effects if the matrix ion is heavy it has more kinetic energy and will stay closer to the center of the ion beam where it forces lighter

analyte ions away from the beam to a greater extent. Subsequently analyte ions will not reach the detector, resulting in a signal less than expected for a given analyte concentration. A computer simulation of this phenomenon is shown in (figure 12). These observations largely point to matrix effects resulting from the mass spectrometry process.

Because of the relationship of the amount of matrix ion in the ion beam and the magnitude of the interference, creative selection of plasma conditions to limit the number of matrix ions can reduce matrix effects. Tan and Horlick [32] adjusted the sample gas flow rate such that a 1000 ppm Cs matrix only suppressed the Sc analyte signal 20%. While changing plasma conditions can occasionally help reduce the severity of matrix effects, almost any change made to the plasma in this manner will result in a loss of sensitivity for the analyte. Modern instruments often have great enough sensitivity that some loss is not too detrimental.

Flow Injection in ICP-MS

The exploration of coupling flow injection (FI) to ICP began in the early 1980s [26]. FI can have many different forms, but essentially a small volume (generally 20-200 µl) of sample is injected into a carrier stream and forms a zone that is transported to the detector. Between the time of injection and detection the sample zone can undergo separation or chemical reaction if desired. Other benefits of this type of analysis are reduced sample consumption and waste management costs, ease of automation, and high sample throughput.

Of particular interest in this dissertation is the ability of FI to allow for the analysis of complex samples [26]. Some examples include analysis of undiluted blood serum by McLeod's [33]. By injecting 20 µl samples and using a higher RF power, interferences were

minimized over continuous flow sampling. Beauchemin [34] determined Mo in seawater using standard additions in conjunction with FI.

Introduction of only a discrete plug of sample solution by FI attenuates cone clogging [35, 36] which can be a cause of signal drift in ICP-MS. Memory effects are also reduced by FI, and sample rinse-out times are shortened. To achieve these benefits the experiments presented in Chapter 3 used an ESI SC-2 FI autosampler (figure 13). This system uses a vacuum pump to quickly deliver sample to the loop. The use of the vacuum system also eliminates sample contact with the peristaltic pump tubing which again reduces memory effects. The injection valve of this system is computer controlled and the injection times are variable in these experiments so the injection volumes are not controlled directly as would normally be the case. A schematic of the FI setup is shown here (figure 14).

Shielded Torch in ICP-MS

The torch system described in the "fundamental" section of Chapter 1 is an unshielded torch. Another popular system is the shielded torch in which a grounded metal cylinder is placed between the torch and the load coil (figure 15). This shield prevents capacitive coupling between the load coil and the plasma, reducing the plasma potential as well as secondary discharge. This reduction in potential enables optimum interferences removal and better ion beam focusing [37]. Removing secondary discharge prevents the re-ionization of polyatomic which can cause spectral interferences. The sensitivity of the HP 4500 in shielded mode is approximately 3 times greater than without.

Dissertation Objectives and Organization

The main body of the dissertation is made up of Chapters 2 and 3, each of which is a complete scientific manuscript. These manuscripts contain their own references, figures, and tables. Chapter 4 is a general conclusion of significant outcomes of this work and poses future work to be done on these subjects.

Chapter 2 describes the designing and subsequent validation of an EMLC column for the express purpose of cleaning ICP-MS blanks. An EMLC column constructed of largely inert materials and with low pressure pumping requirements is produced. When potential is applied to the column many contaminant elements in acid blanks are removed to near D.I. water concentrations. These low blank signals could potentially improve the limit of detection for the instrument for certain specialty applications. Graduate student Cory T. Gross is the primary researcher/author and Professor R.S. Houk was an advisor and corresponding author.

Chapter 3 describes the study of the fast flow injection analysis of high matrix solutions and the matrix effects observed. A flow injection system is coupled to an ICP-MS with an unshielded torch to analyze a range of analytes with several different matrix elements. In most cases the signal recovery is much better than typically observed; even analytes in undiluted seawater experience only ~25% suppression. The results raise some questions about the nature of matrix effects. Graduate student Cory T. Gross is the primary researcher/author and Professor and R.S. Houk was an advisor and corresponding author along with Professor Marc D. Porter.

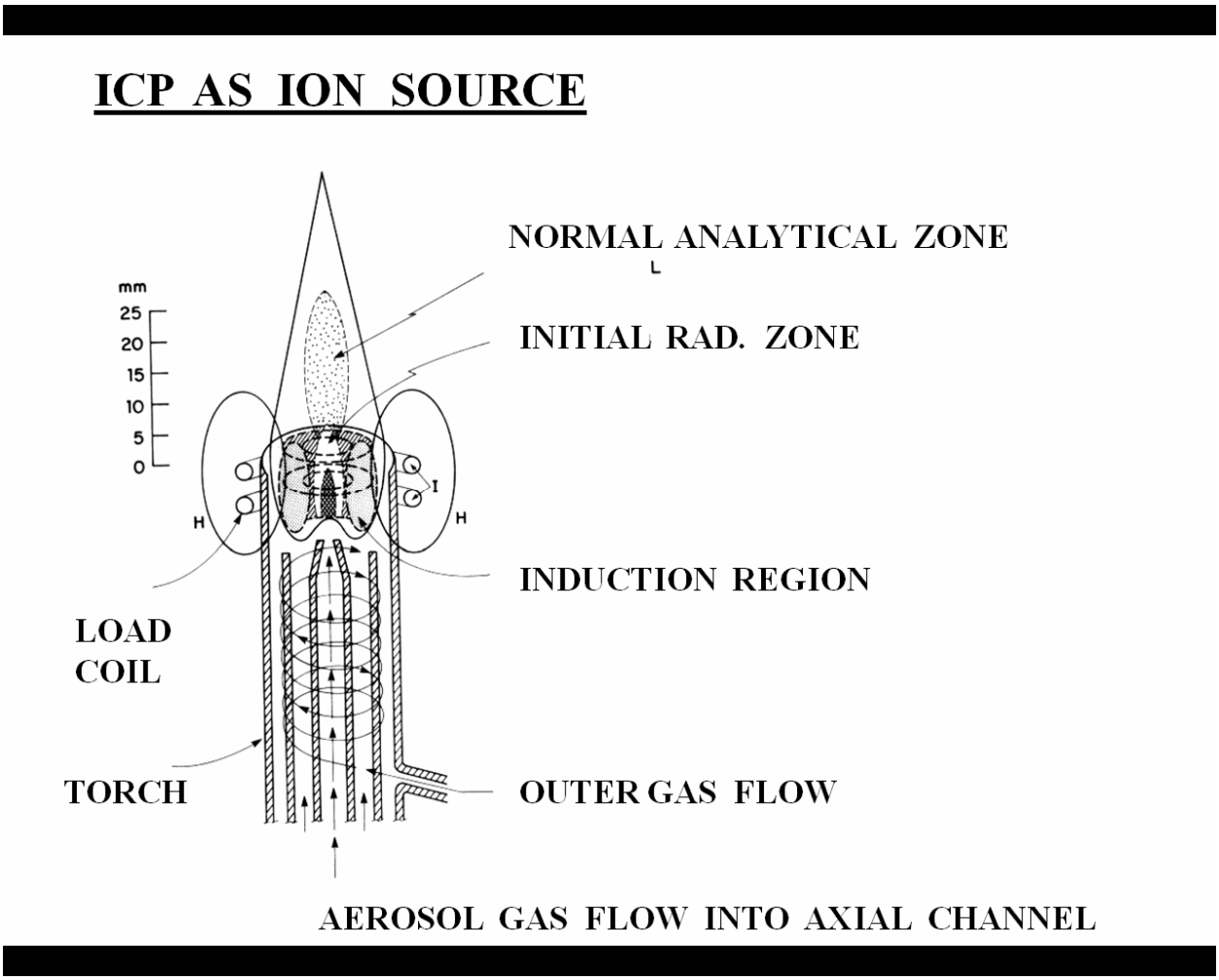

Figure 1. Schematic of a Fassel torch [38].

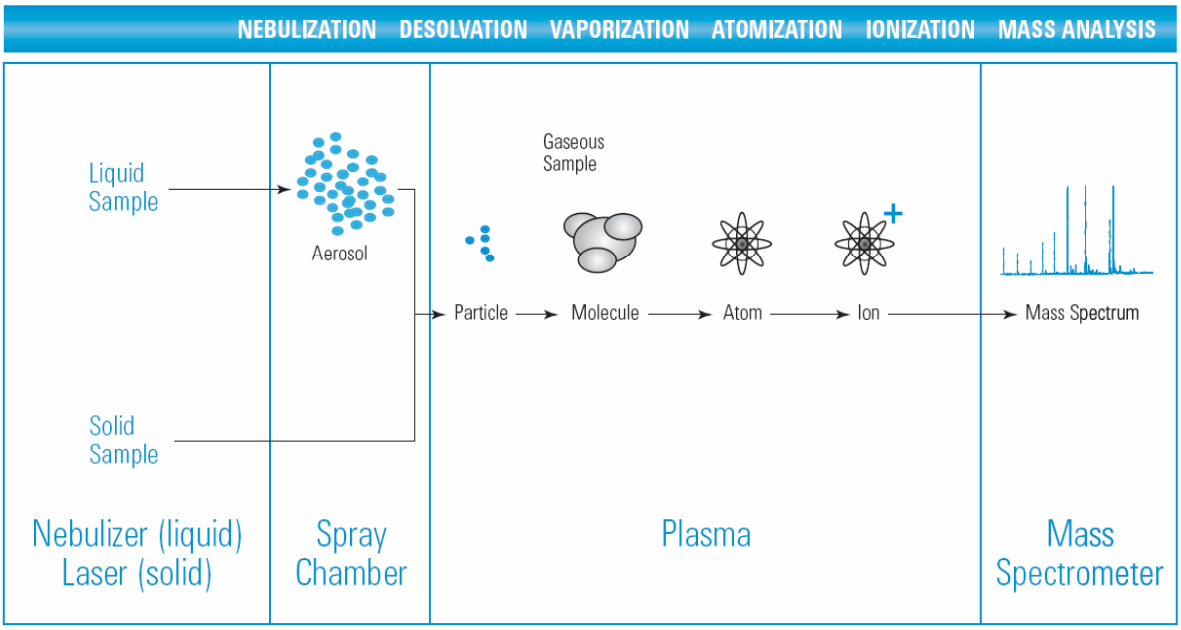

Figure 2. Schematic of the sample path through an ICP-MS instrument [39].

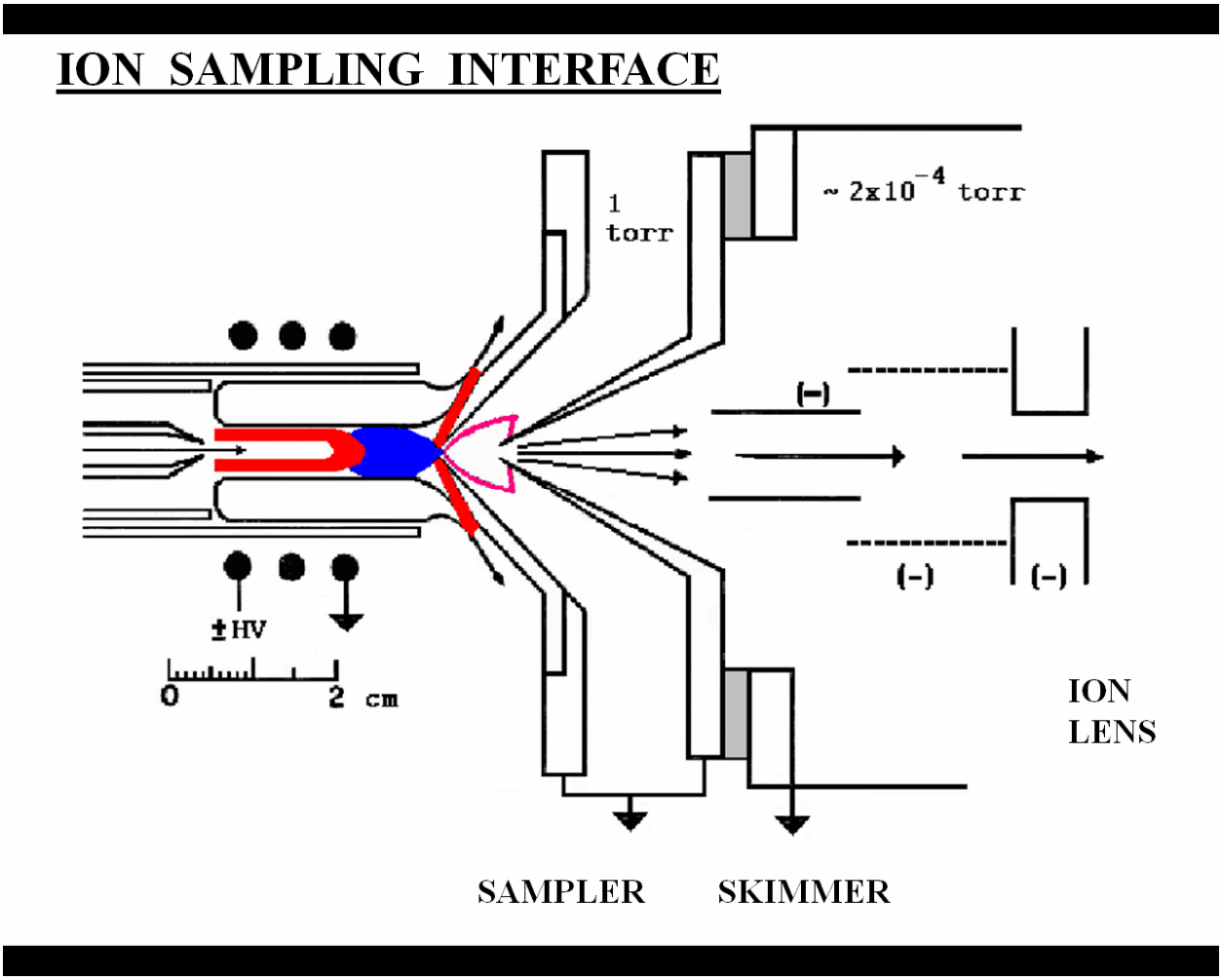

Figure 3. Schematic of the ICP-MS interface [40].

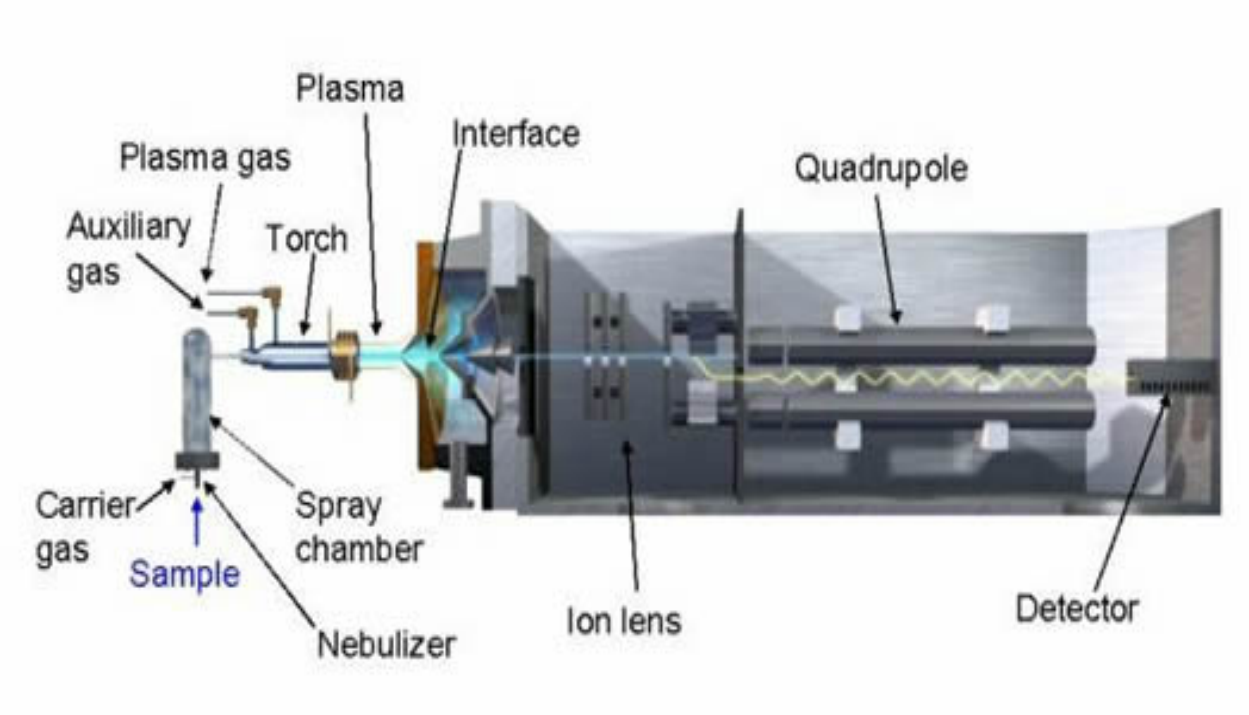

Figure 4. Schematic of the HP 4500 series ICP-MS [41].

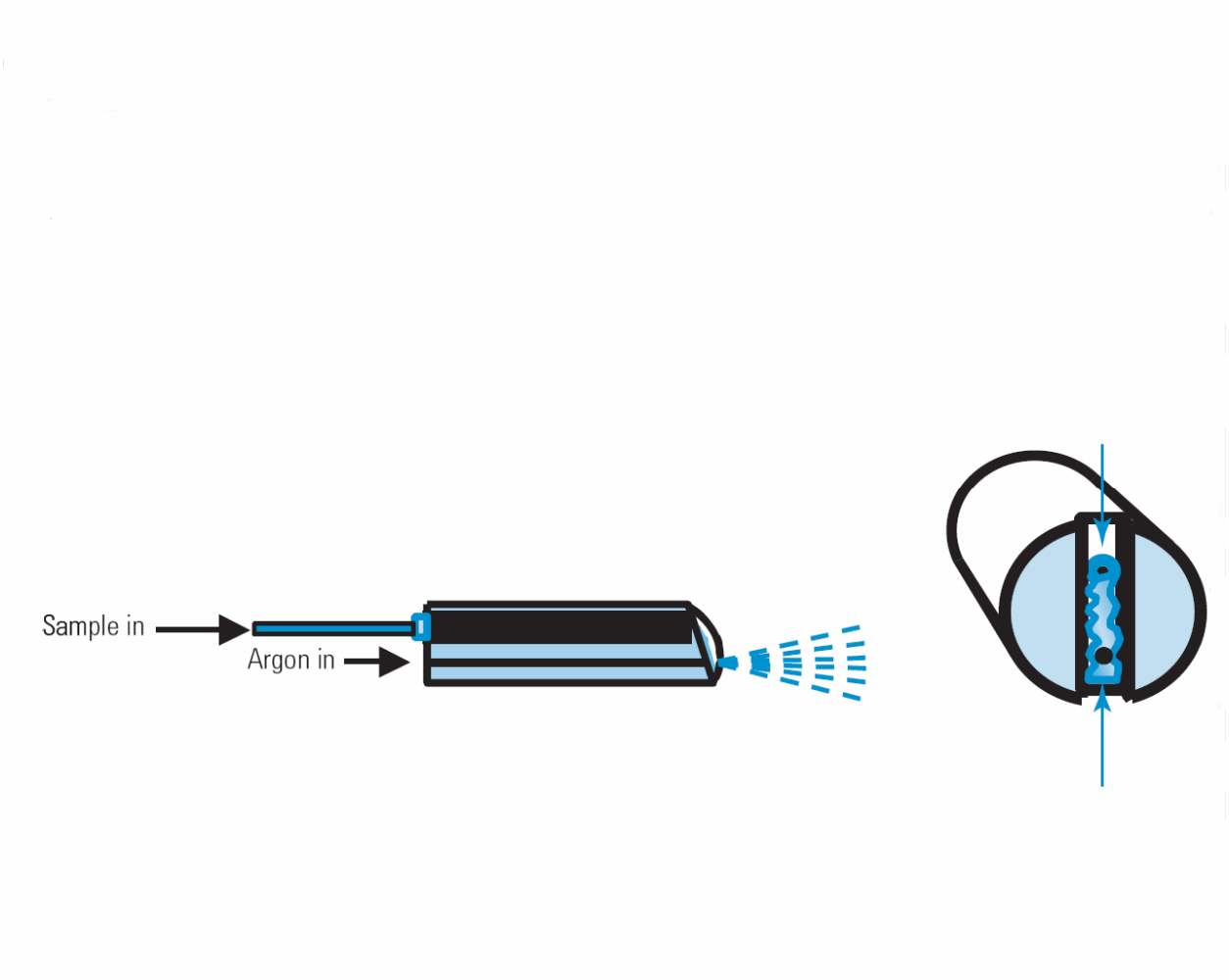

Figure 5. Schematic of the Babington nebulizer [39].

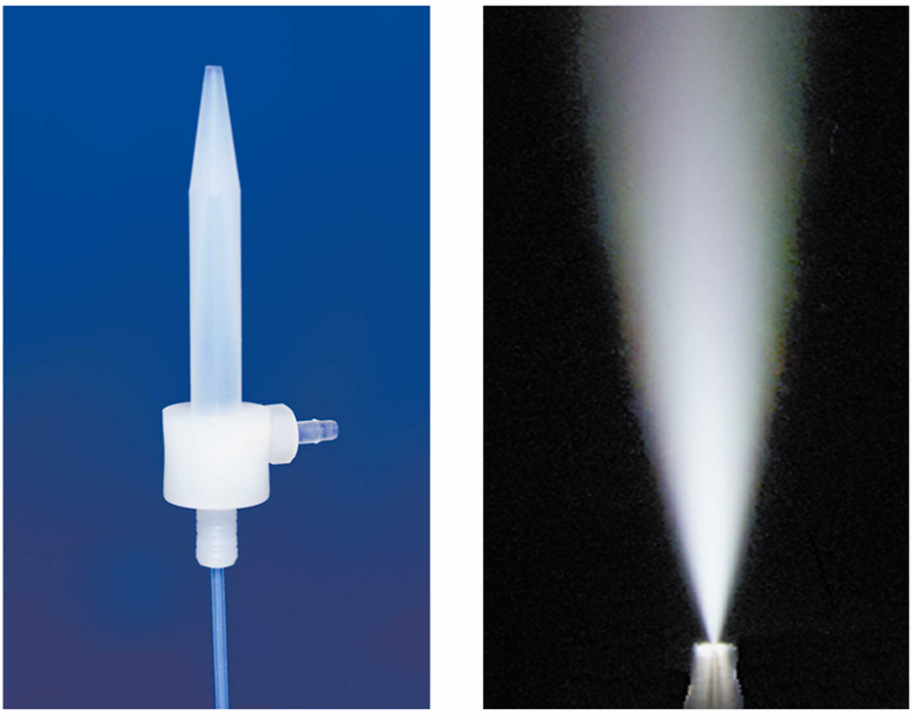

Figure 6. PFA micro concentric nebulizer [42].

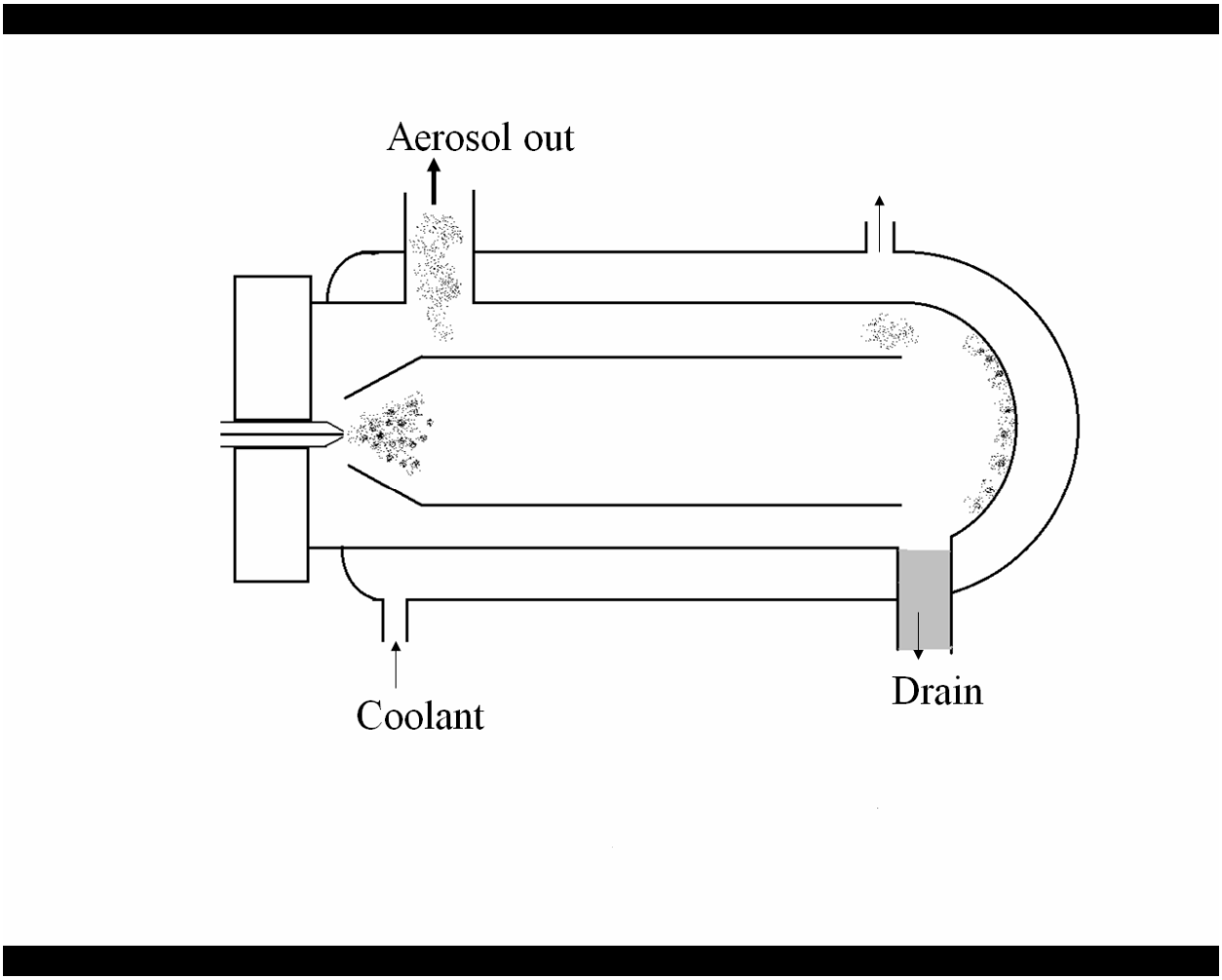

Figure 7. Schematic of a double-pass Scott type spray chamber [40].

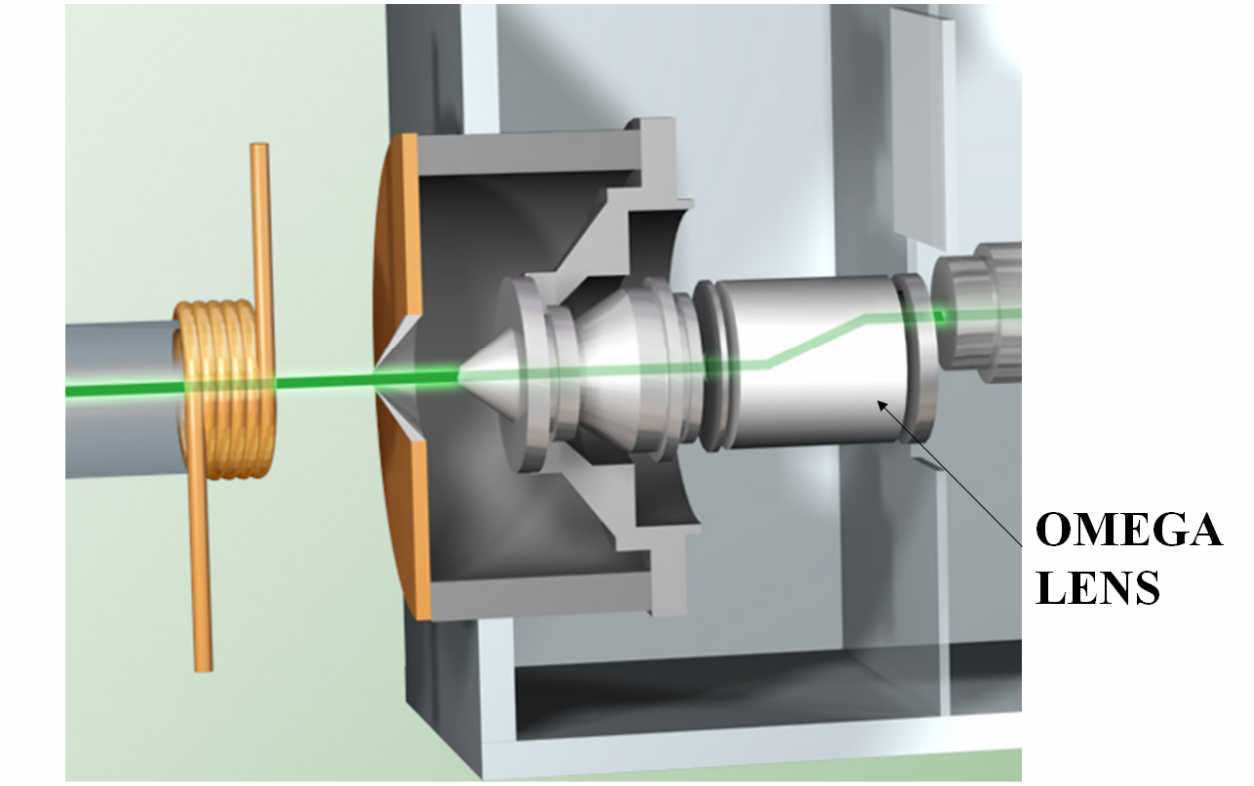

Figure 8. Schematic of Omega lens [41].

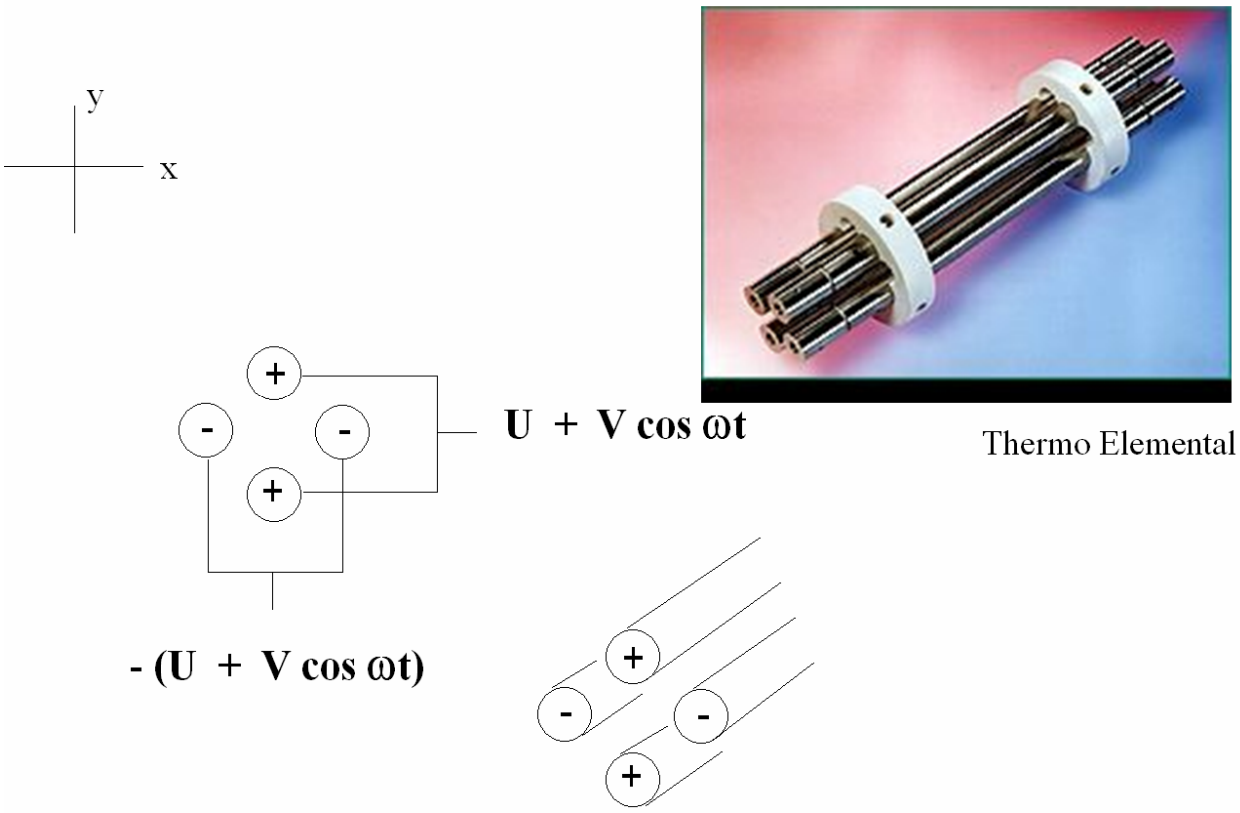

Figure 9. Quadrupole mass analyzer [43].

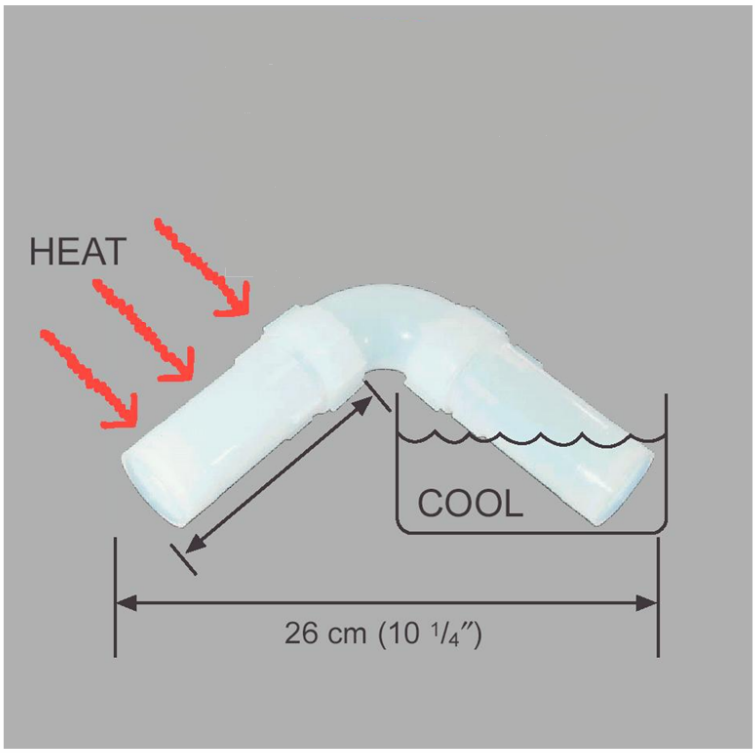

Figure 10. Teflon sub-boiling distillation apparatus (Sallivex, Minnetonka, MN) [40].

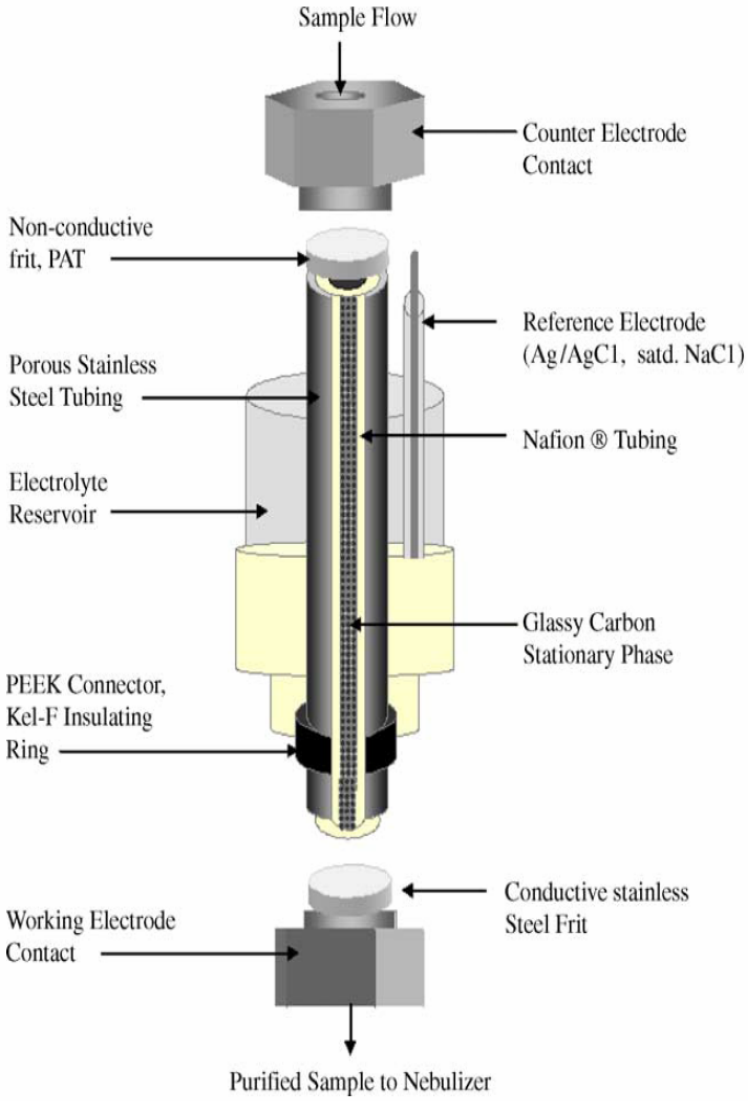

Figure 11. Original version of EMLC column [5]

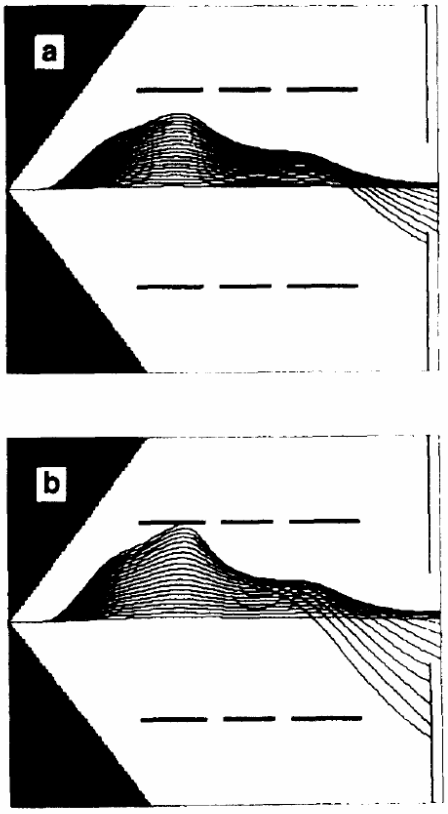

Figure 12. Effect of space charge on trajectories of $24Mg^{+}$ behind skimmer and through ion lens. The inside wall of the skimmer is shown at the left of each frame, and only half of the full view is shown. (a) Mg- trajectories from matrix-free solution; (b) a 1% thallium matrix broadens the Mg^{+} beam, and fewer Mg^{+} ions pass through the aperture at the right [25] .

Figure 13. ESI SC-2 autosampler [42].

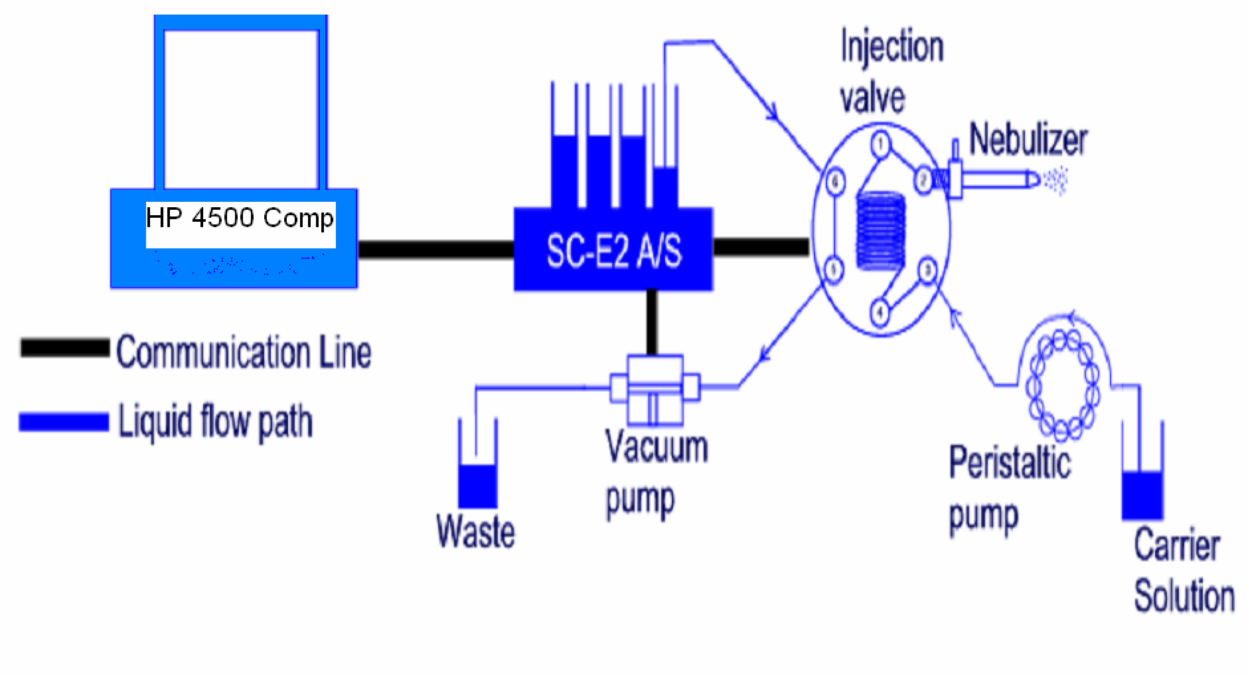

Figure 14. Schematic of flow injection system [42].

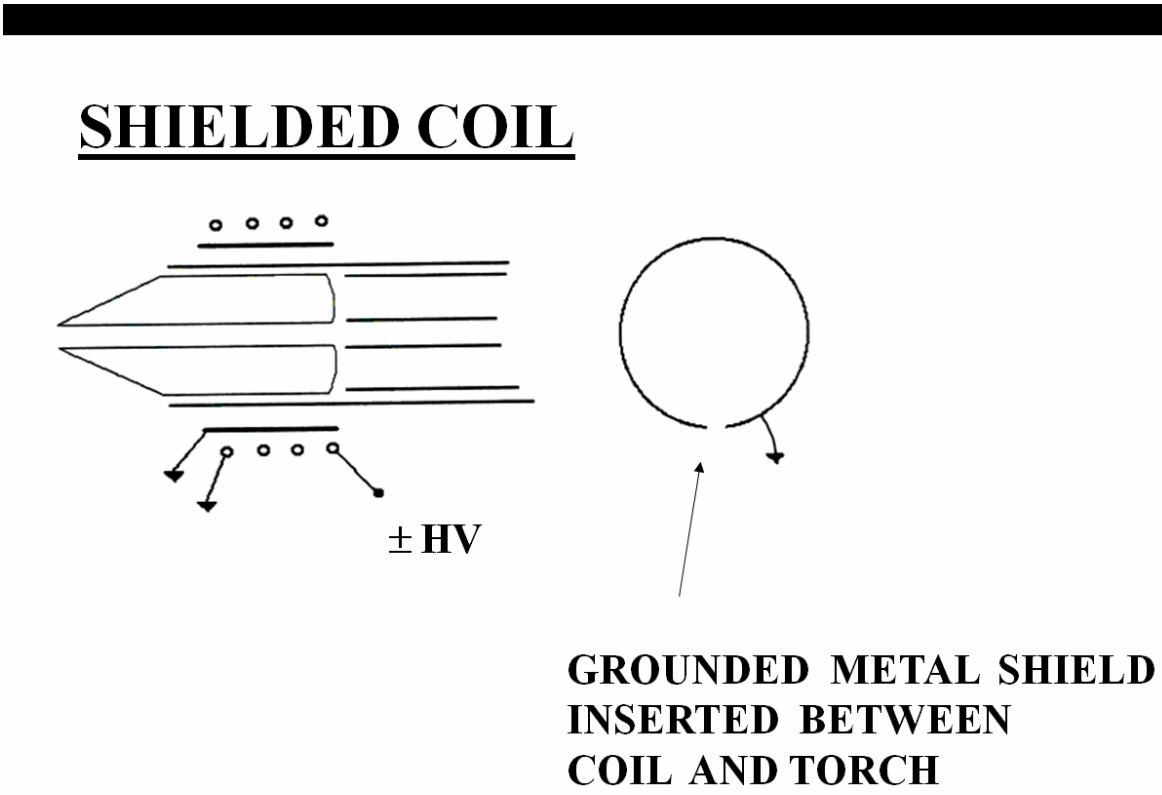

Figure 15. Schematic of a shielded torch [40].

References

1. Greenfield, S.; Jones J.L.; Berry, C.T. *Analyst*, **1964**, 89, 713

2. Wendt, R.H.; Fassel, V.A. *Anal. Chem.*, **1965**, 37, 920

3. Gray, A.L. *Proc. Soc. Anal. Chem.*, **1974**, 11, 182-183

4. Gray, A.L. *Analyst*, **1975**, 289-299

5. Houk, R.S.; Fassel, V.A.; Flesh, G.D.; Svec, H.J.; Gray, A.L.; Taylor, C.E. *Anal. Chem.*, **1980**, 52, 2283

6. Jarvis K.E.; Gray, A.L.; Houk, R.S. Handbook of Inductively Coupled Plasma Mass Spectrometry, Chapman and Hall, New York, 1992

7. Mallinckrodt Baker (J.T. Baker) online catalog (www.mallbaker.com)

8. Kuehner, E.C.; Alvarez, R.; Paulsen, P.J.; Murphy, T.J. *Anal. Chem.*, **1972**, 44, 2050-2056

9. Moody, J. R. *Philos. Trans. R. Soc. London*, **1982**, 305, 669-680

10. Hasan, Towhid; Gazda, Daniel, Gazda; Porter, Marc D.; Houk, R.S. *Anal. Chim. Acta*, **2005**, 537, 63-68

11. Ting, En-Yi; Porter, Marc D. *Anal. Chem.*, **1998**, 94-99

12. Ponton, Lisa; Porter, Marc D. *Anal. Chem*., **2004**, 76, 5823-5828

13. Ponton, Lisa; Porter, Marc D. *J. Chromatogr. A*, **2004**, 1059, 103-109

14. Deng, Haiteng; Van Berkel, Gary J.; Takano, Hajime; Gazda, Daniel; Porter Marc D. *Anal. Chem.*, **2000**, 72, 2641-2647

15. Hongsen, N.; Houk, R.S. *Spectrochim. Acta, Part B*, **1996**, 51, 779-815

16. Olivares, J.A.; Houk, R.S. *Anal. Chem.*, **1988**, 58, 20-25

17. Crain, J.S.; Houk, R.S.; Smith, F.G. *Spectrochim. Acta, Part B*, **1989**, 44, 1355

18. Tan, S.; Horlick, J. *Anal. Atomic Spectrom.*, **1987**, 2, 745

19. Evans, E.H.; Giglio, J.J. *J. Anal. Atomic Spectrom.*, **1993**, 8, 1

20. Gregoire, D.C. *Appl. Spectosc.*, **1987**, 41, 467

21. Vandecasteele, C.; Nagels, M.; Vanhoe, H.; Dams, R. *Anal. Chim. Acta*, **1998**, 211, 91

22. Kawaguchi, H.; Tanaka, T.; Nakamura, T.; Morishita, M.; Mizuike, A. *Anal. Sci.*, **1987**, 3, 305

23. Hobbs, S.E.; Olesik, J. *Appl. Spectrosc.*, **1991**, 45, 1395

24. Lazar, A.C.; Farnsworth, P.B. *Appl. Spectrosc.*, **1999**, 53, 465-470

25. Beauchemin, D.; McLaren, J.W.; Berman, S.S *Spectrochim. Acta, Part B*, **1987**, 42, 467

26. Montaser, A. (Ed.), Inductively Coupled Plasma Mass Spectrometry, VCH, New York, 1996

27. Taylor, H.E.; Gabrino, J.R., Analytical Applications of ICP-MS, in Monstaser A.; Golightly, D.W. (Eds.) Inductively Coupled Plasmas in Analytical Atomic Spectroscopy, 2nd edn., VCH, New York, 1992, Chap. 14.

28. Tanner, S.D. *Spectrochim. Acta, Part B*, **1992**, 47, 809

29. Gillson, G.R.; Douglas, D.J.; Fulford, J.E.; Halligan, K.W.; Tanner, S.D. *Anal. Chem.*, **1988**, 60, 1472

30. Li, G.; Duan, Y.; Heiftje, G.M. *Mass Spectrom.*, **1995**, 30, 841

31. Chen, X.; Houk, R.S. *Spectrochim. Acta, Part B*, **1996**, 41, 516

32. Tan, S.; Horlick, J. *Anal. Atomic Spectrom.*, **1987**, 2, 745

33. McLeod, C.W.; Worsfold, P.J.; Cox, A.G. *Analyst*, **1984**, 109, 327-332

34. Beauchemin, D. *Anal. Chem.*, **1995**, 67, 1553-1557

35. Thompson, J.J.; Houk, R.S. *American Mineralogist*, **1982**, 67, 238-243.

36. McClenathan, D.M.; Ray, S.J.; Hieftje, G.M. *J. Anal. Atomic. Spectrom.*, **2001**, 16, 987-990.

37. HP 4500 Chemstation Operater's Manual

38. Fassel, V.A. *Pure. Appl. Chem.*, **1977**, 49, 1533

39. ICP-MS Principles and Hardware manual, Agilent Technologies, 2005

40. Houk, R.S., ICP-MS Short course

41. Agilent Technologies online resources (www.agilent.com)

42. Elemental Scientific Inc. online product catalog (www.elementalscientific.com)

43. Thermo Scientific online resources (www.thermo.com)

Chapter 2. Electrochemically-Modulated Liquid Chromatography for Cleaning the Blank in Inductively Coupled Plasma – Mass Spectrometry

A paper to be submitted to the *Journal of Analytical Atomic Spectrometry*

Cory T. Gross, Marc D. Porter[a] and R. S. Houk

Ames Laboratory – U. S. Department of Energy
Department of Chemistry, Iowa State University, Ames IA 50011 USA

[a]Present address: Department of Chemistry, University of Utah, Salt Lake City UT 84112-0850 USA

Abstract

A metal-free, low-pressure, electrochemically modulated liquid chromatography (EMLC) column was evaluated specifically for use on-line with ICP-MS. The stationary phase is reticulated vitreous carbon (RVC), and the reference and counter electrodes are positioned upstream from the column to minimize contamination. The EMLC column reduces levels of trace elements in blank solutions just before the blank is introduced into the nebulizer. Many metal ions can be removed at a single applied potential of ~-0.75 V (vs SHE). Favorable elements are removed to count rates of 5 to 100 counts/s, close to the blanks from deionized water for the instrument used.

Introduction

Detection limits are a strength of ICP-MS. With the sensitivity of today's ICP-MS instrumentation, detection limits are often limited by the cleanliness of the blank [1,2]. In order to work at the lowest concentrations, it is desirable to remove the trace metal contaminants that are common in ICP-MS blanks, which are generally aqueous acids of various types and concentrations.

Several techniques are commonly used to produce low blanks. Water can be made very pure by methods like reverse osmosis. Acids are purchased in high purity and/or purified prior to use by sub-boiling distillation [3]. While sub-boiling distillation is effective in removing many undesirable contaminants, the boiling points of some elements are low enough that it is not an effective means of removal, particularly Hg and As. Sub-boiling distillation is also slower and less effective on acids with high boiling points such as sulfuric acid.

Conceivably, these off-line, batch methods could be combined with an on-line purification column to clean the blank directly before use. This would reduce re-contamination upon storage. Sanz-Medel and co-workers describe such a chelating column for on-line cleanup of eluents for liquid chromatography [4]. The acids commonly used for elemental analysis would protonate most chelating agents, thus reducing their ability to remove the elements of interest.

We previously described use of an EMLC column for cleanup of aqueous acids [5]. This column was effective enough to demonstrate the concept but was originally designed for

chromatographic analysis [6], hence it was housed in stainless steel and required a high pressure LC pump. The latter generated unnecessary noise in the ICP-MS signal.

This paper describes an EMLC column specifically designed for cleanup of acid blanks for ICP-MS. The new column is housed in Teflon to minimize metal contamination. Electrode material is also an important consideration. The reticulated vitreous carbon (RVC) used as the working electrode in this column is rigid, porous, has high surface area, and is easily "packed" into the column. A low pressure pump is adequate, resulting in a less noisy signal and therefore better blank standard deviation. The column works effectively for removal of metal interferences at flow rates and back pressures conducive to ICP-MS analysis.

The primary principle believed to be at work in the metal removal process is similar to that of anodic stripping voltametry. The working electrode is held at a potential generally more negative than the reduction potential of the elements to be removed. As the metals encounter the working electrode they are electrodeposited. After the desired blank signal is obtained, the metals can be released easily from the column by switching the applied potential to an appropriately positive value. Carbon electrodes are also effective for preconcentration of metallic analytes such as Pt and U in a similar on-line manner, as shown by Caruso [7-9], and Van Berkel, Duckworth and co-workers [10, 11]. The present work differs in that the stripping process is used to cleanse the blank, not retain the analyte.

Experimental

Instrumentation. These experiments were performed on an Agilent HP 4500 series single quadrupole ICP-MS with no collision cell. The sample is transported via an on-board peristaltic pump, which provide adequate pressure for pumping through the column. A Babington nebulizer and a double pass Scott type spray chamber are employed. The instrument parameters are tuned for optimal sensitivity and the liquid flow rate is set at approximately 100 μL/min. Important operating parameters are shown in Table 1.

The EMLC column (Fig. 1) functions as a three-electrode electrochemical cell. The working electrode is a porous RVC cylinder (radius 0.5 cm x 5 cm long , 100 pores per linear inch, pore size ~ 0.25 mm, ERG Materials and Aerospace Corp., Oakland, CA) that fits snugly inside the Teflon housing. The counter electrode is a Pt grid (wire diam. ~0.9 mm, 0.5 x 1 cm). Potential is applied to the cell via an external potentiostat (Model 173, Princeton Applied Research, Oak Ridge, TN). For precise control of the applied potential a saturated Ag/AgCl reference electrode is used (for convenience all stated potentials are corrected to that of the standard hydrogen electrode). The working electrode is downstream so that metals from the other two electrodes can be deposited in the working electrode. Electrical connection to the working electrode is achieved through a carbon post inserted through the cylindrical Teflon case into the RVC. For the results shown below, the potential applied to the working electrode is -0.75 V, which works for many elements. The EMLC column is placed on-line after the peristaltic pump and before the nebulizer (Fig 2) .

Solution Preparation. Acid blanks were prepared using concentrated nitric and sulfuric acids (Fisher certified A.C.S. reagent grade plus, Fair Lawn NJ). These acids were diluted to 1% with distilled deionized water (Barnstead Nanopure-II, 18MΩ, Barnstead Co., Newton MA). These acids and concentrations are typical for ICP-MS analysis. Two spiked

solutions of As and Hg were prepared using 1000 mg/L single element standards (Spex Certiprep, Metuchen NJ).

Results and Discussion

Removal of Various Metals from 1% HNO_3. The goal of these experiments is to reduce signals from interfering metals in our blanks to the lowest possible level. Initially the blank is passed through the column at open circuit (no applied potential) while ICP-MS data are collected. Even at open circuit the RVC column removes a small amount of contaminant, suggesting some natural affinity of the metal ions for the carbon substrate.

In the plots shown below (e.g., Fig. 3) the potential is applied at time = zero. The signal for the metal ion in the blank begins to drop after 500 to 800 s. This delay is attributed to the dead volume in the column and to the time required for the working electrode to charge to the desired potential. This delay is encountered only at the beginning of a day's experiments. After the deposition process begins at ~ 670 s, the signal falls rapidly, within ~ 50 s.

Figures 3 and 4 show representative results for removal of Pb and Zn from 1% HNO_3. The potential on the working electrode is -0.75 V; other potentials were tested, this one was best. In Fig. 2, the $^{208}Pb^{+}$ signal is attenuated from 36,000 counts/s to ~ 75 counts/s, a factor of 480. For Zn (Fig. 2), the signal at m/z = 66 is much lower initially (600 counts/s) and is also attenuated to ~ 75 counts/s, about the same level as that for lead. On this particular instrument, deionized water gives signals of about this magnitude for these common

elements. This suggests that the removal factors could be improved further if the rest of the instrument could be kept cleaner.

The results of similar experiments for various elements in 1% HNO_3 are given in Fig. 5 and Table 2. At an applied potential of -0.75 V, many metals are removed to count rates of 5 to 100 counts/s. This is a key point for multielement analysis, the usual application of ICP-MS. Three exceptions are Fe, Mn and Ag. Iron and Ag should be deposited at -0.75 V. We suspect the signal at m/z = 57 is actually mostly polyatomic ion instead of $^{57}Fe^{+}$. The Ag level is better than in the previous experiments [5] and could be due to inability to completely remove contamination from the reference electrode. We did not notice evidence of H_2 evolution at -0.75 V; this process is expected at potentials more negative than -0.83 V [5]. All the elements shown in Table 2 are purged if the column potential is changed to +0.75 V; this is seldom necessary.

Removal of Various Metals from 1% H_2SO_4. Table 3 shows analogous results for removal of multiple elements from 1% H_2SO_4. For most elements, the column reduces signals to about the same levels as with 1% HNO_3. Silver is removed better in this case, Fe and Mn signals are still not attenuated much.

Removal of Various Metals from 2% HCl. Table 4 summarizes the results for removal of multiple elements from 2% HCl which is another fairly common acid used for dissolution. HCl was found to have a more V, Cr, Zn, and As than the acids previously described. In particular the removal of Cr was well demonstrated in this case with a reduction in signal of 400 times.

Removal of Metals from Higher Concentrations of Acid. While acids of 10% concentration may not be common as acid blanks, cleaning of these acids for later dilution may be useful. The results for 10% nitric are shown in Table 5 and 10% sulfuric in Table 6. As expected the starting concentration of contaminant elements is generally greater than the 1% counterpart, although not usually 10 times greater. This is likely due to some loss of sensitivity at these operating conditions from higher acid concentrations. Testing of higher concentration acids also demonstrates the robustness of the system, although parts of the ICP-MS should not be subjected to large amounts of concentrated acid due to possible damage of the sample introduction system and cones.

Removal of As and Hg. The initial levels of As and Hg in either 1% HNO_3 or 1% H_2SO_4 are quite low (Tables 2 and 3). These elements have volatile forms that can pose problems for sub-boiling distillation. Thus, these elements were spiked into 1% HNO_3 solutions to test the ability of the column to remove them.

These results are shown in Figs. 6 and 7. Only the latter part of the acquisition is shown; data obtained during the initial equilibration/charging time are the same as in previous figures and are not plotted. For $^{75}As^{+}$ the blank is reduced from 2400 to 150 counts/s; 40,000 counts/s for $^{202}Hg^{+}$ are attenuated to 400 counts/s. The removal factors are 16 and 100 for $^{75}As^{+}$ and $^{202}Hg^{+}$, respectively. As before, the removal factor is larger the higher the initial count rate of the element.

Conclusion

EMLC is shown to be a valuable supplement to the cleaning techniques for getting the very cleanest acid blanks. Signal levels near those of D.I. water are demonstrated for many of the contaminant elements found in typical acid blanks, including elements like As and Hg, for which sub-boiling distillation is less effective. Contaminant removal and cleaning of the column is conveniently controlled by the simple changing of potential. Improvements could be made to the design to lessen the dead volume as well as increasing the initial flow rate to improve response times as nearly 700 s demonstrated may not be acceptable in all cases. Substituting a different reference electrode would also be advisable if Ag was of particular concern in a given experiment. This technique should be applicable to any solution with enough supporting electrolyte thus acids of varying concentrations can be cleaned with no modification. Further studies may involve contaminant removal from organic solvents with supporting electrolyte added.

Acknowledgements

The authors thank Agilent for donating the ICP-MS instrumentation used in this research. Funding was provided by the Chemical and Biological Sciences Program, Office of Basic Energy Sciences, Ames Laboratory U. S. Department of Energy under Contract No. DE-AC02-07CH11358.

References

1. Yuan, H.; Hu ,S.; Tong, J.; Zhao, L.; Lin, S.; Gao, S. *Talanta*, **2000**, 52, 971- 981

2. Richter, R. *Spectroscopy*, **2001**, 16, 21-24

3. Kuehner, E.; Alvarez, R.; Paulsen, P.; Murphy, T. *Anal. Chem.*, **1972**, 44, 2050-2056

4. Cabezuelo,A.B.; Montes-Bayon, M.; Garcia Alonso, J.I.; Sanz-Medel, A. *Analyst*, **1988**, 123, 865

5. Hasan, T.; Gazda, D.; Porter, M.D.; Houk, R.S. *Anal. Chim. Acta* **2005**, 537, 63-68

6. Ting, E.Y.; Porter, M.D. *Anal. Chem.*, 1998, **70**, 94-99; Ponton, L.; Porter, M.D, *Anal. Chem*., 2004, **76**, 5823-5828; *J. Chromatogr. A*, **2004**, 1059, 103-109

7. Pretty, J.R.; Evans, E.H.; Blubaugh, E.A.; Shen W.L.; Caruso, J.A. *J. Anal. Atomic Spectrom*. **1990**, 5, 437-443

8. Pretty, J.R.; Blubaugh, E.A.; Evans, E.H.; Caruso, J.A.; Davidson, T.M. *J. Anal. Atomic Spectrom*. **1992**, 7, 1131-1137

9. Pretty, J.R.; Caruso, J.A. *J. Anal. Atomic Spectrom*. **1993**, 8, 545-550.

10. Pretty, J.R.; Duckworth, D.C.; Van Berkel, G.J. *Anal. Chem.* **1998**, 70, 1141-1148

11. Clark, W.J.; Park, S.H.; Bostick,D.; Duckworth, D.C.; Van Berkel, G.J. *Anal. Chem.*, **2006**, 78, 8535-8542

1. **Table 1. ICP-MS Operating Parameters**

Forward power	1200 W
Argon gas flow rates (L/min):	
Outer	14
Auxiliary	1.5
Sample	1.0
Sampler cone	Nickel
	1.1 mm hole diam.
Skimmer cone	Nickel
	0.4 mm hole diam.
Sampling	8 mm from load coil
Position	On center
Ion optics	
Extract 1	-221 V
Extract 2	-66 V
Einzel 1, 3	-125 V
Einzel 2	+15 V

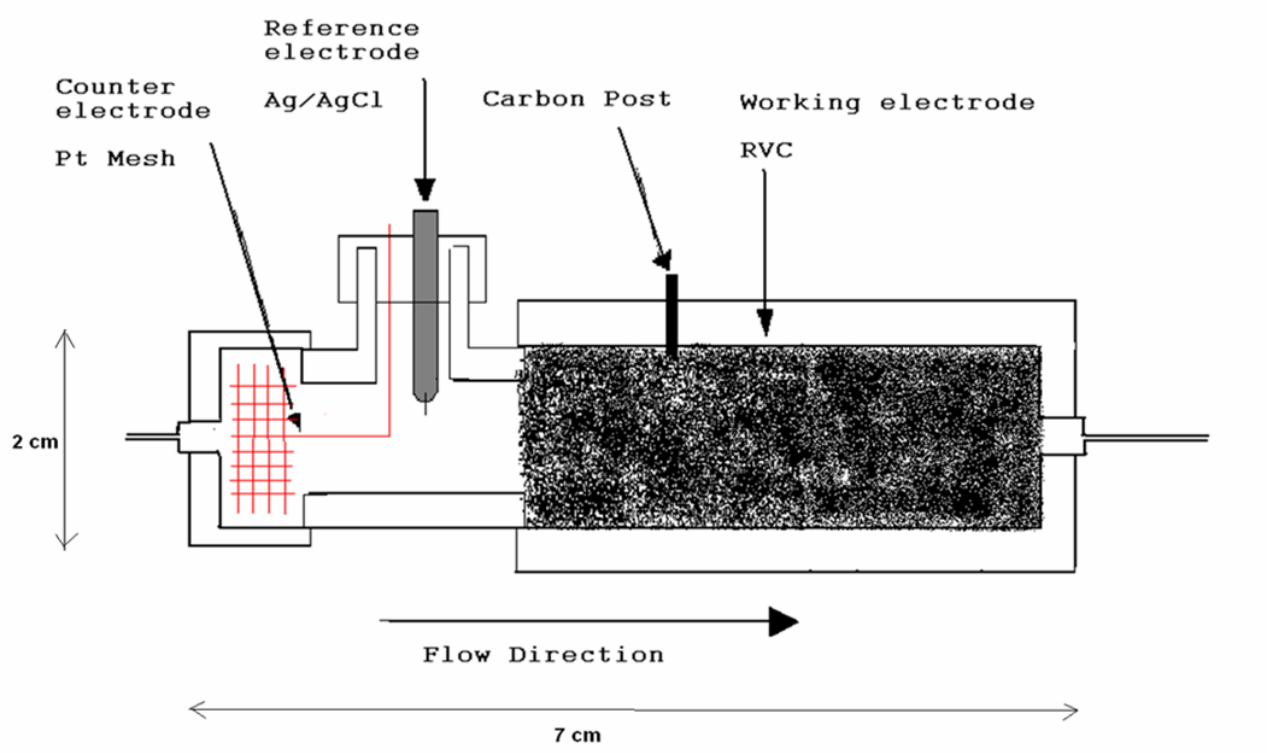

Fig. 1. Schematic diagram of EMLC column.

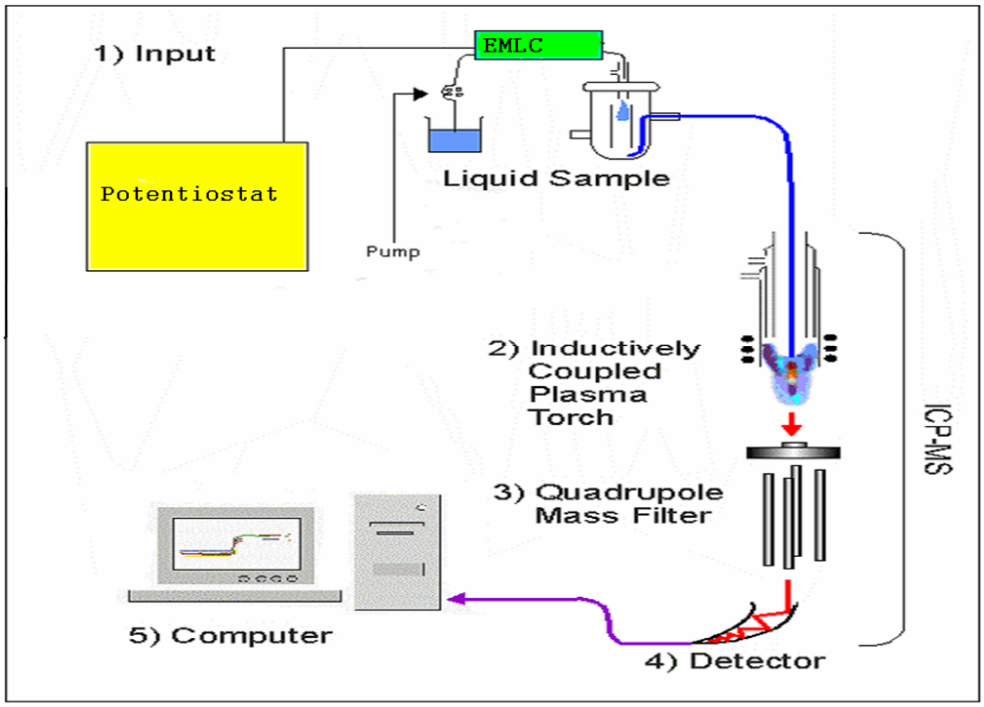

Fig. 2. Schematic of the overall EMLC, ICP-MS setup.

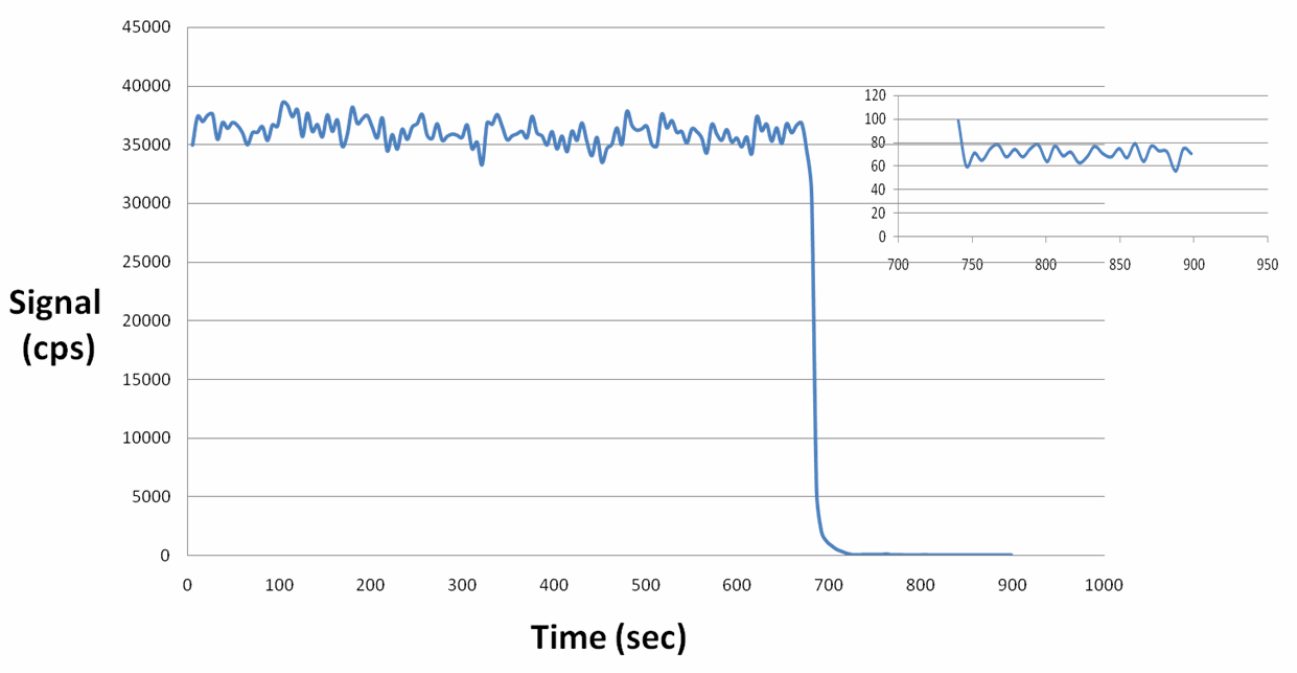

Fig. 3. Signal for $^{208}Pb^{+}$ from 1% HNO_3 vs time. The applied voltage (-0.75 V) was started at time =0; deposition of Pb^{+} begins at ~ 670 s. Inset shows $^{208}Pb^{+}$ signal on more sensitive scale after onset of deposition.

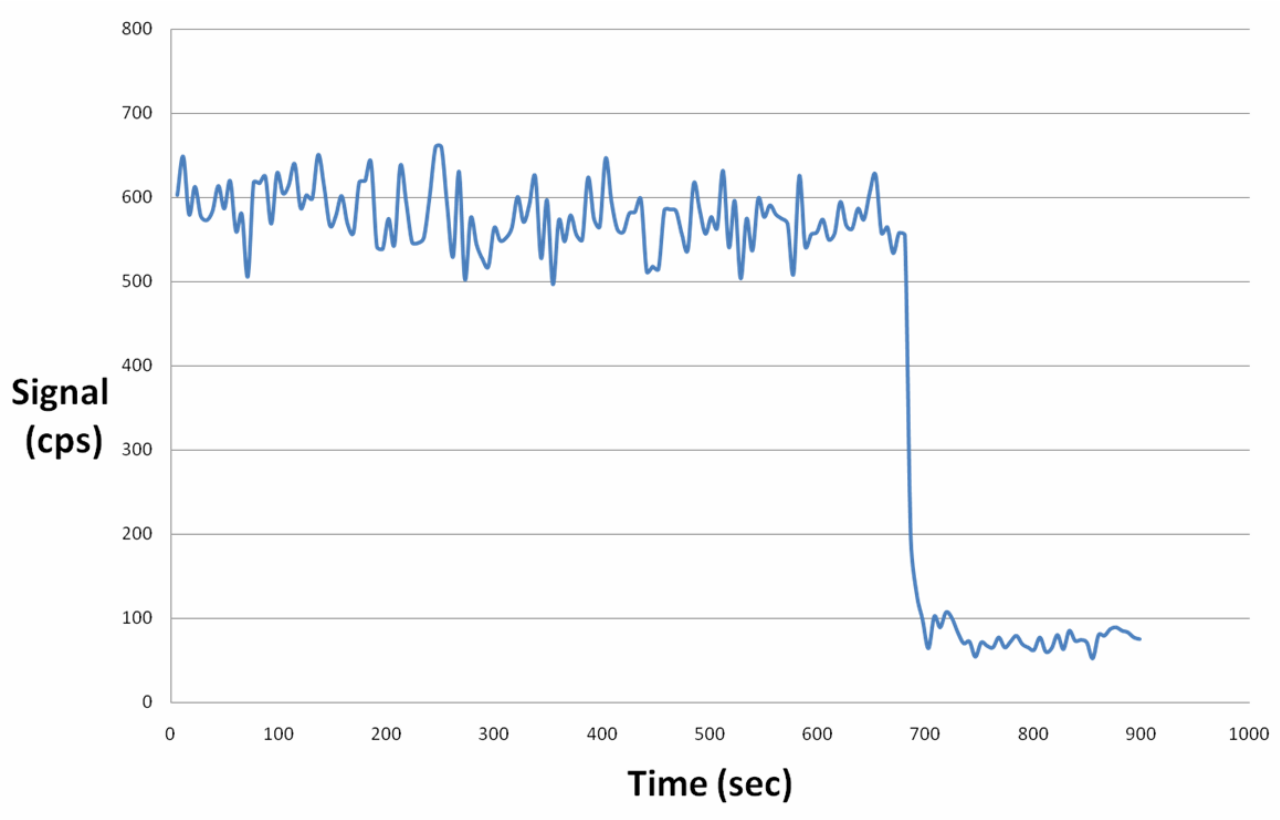

Fig. 4. Signal for $^{66}Zn^{+}$ vs time from 1% HNO_3, -0.75 V on working electrode.

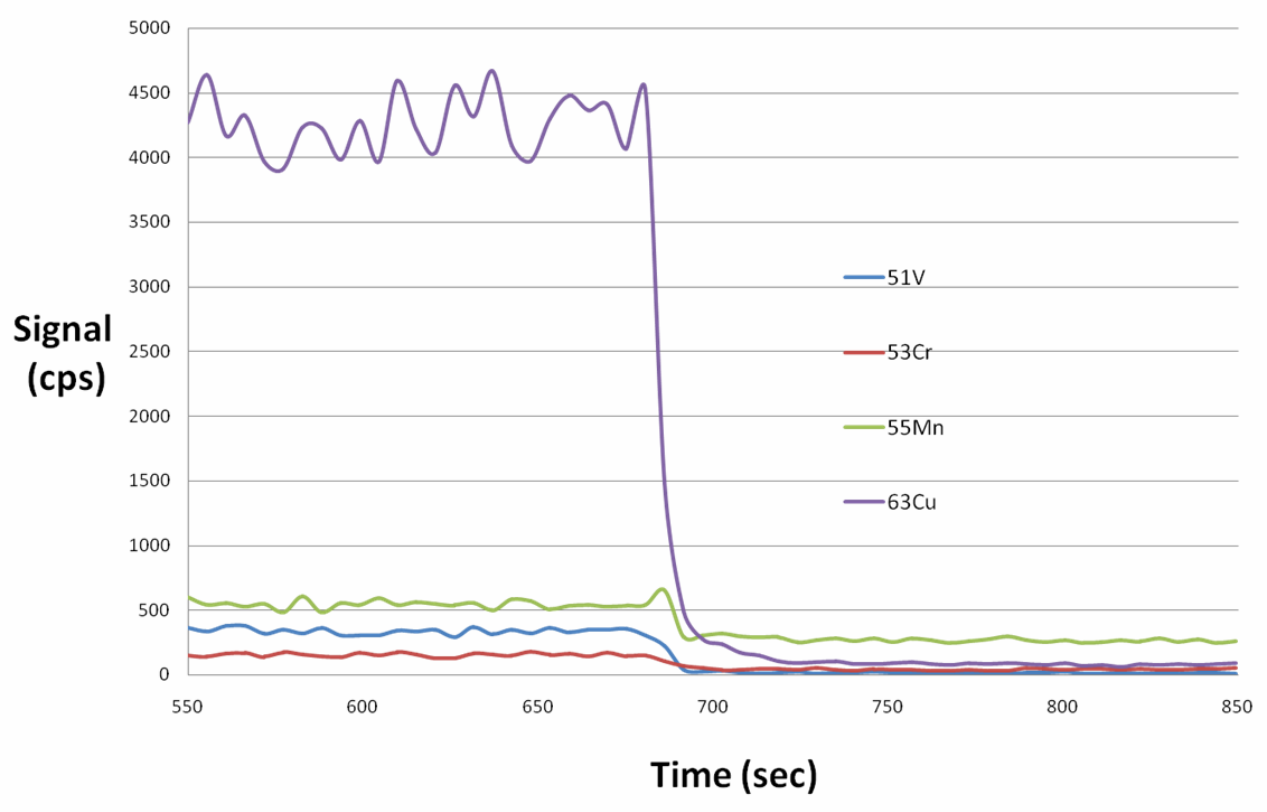

Fig. 5. Removal of multiple elements from 1% HNO_3 with -0.75 V on working electrode.

Table 2. Removal of Elements from 1% Nitric Acid Blank,

-0.75 V Applied to Working Electrode.

	m/z	Initial Signal (c/s)	Final Signal (c/s)	Removal Factor	Final Concentration (ppt)
V	51	350	10	35	5
Cr	53	160	40	4	20
Mn	55	600	250	2.4	125
Fe	57	3500	2500	1.4	1500
Co	59	20	10	2	5
Ni	60	100	30	3.3	15
Cu	63	4500	95	47	50
Zn	66	600	75	8	50
As	75	10	5	2	2.5
Zr	90	50	5	10	2.5
Ag	107	1500	250	6	125
Cd	111	120	90	1.3	45
Sn	118	60	10	6	5
W	182	20	10	2	5
Hg	202	50	35	1.4	17.5
Tl	205	15	5	3	2.5
Pb	208	36000	75	480	50
Bi	209	40	10	4	5

Table 3. Removal of Elements from a 1% Sulfuric Acid Blank, -0.75 V Applied to Working Electrode

	m/z	Initial Signal (c/s)	Final Signal (c/s)	Removal Factor	Final Concentration (ppt)
V	51	2600	25	104	15
Cr	53	100	50	2	25
Mn	55	2000	1500	1.3	750
Fe	57	2700	2400	1.1	1200
Co	59	20	5	4	2.5
Ni	60	500	20	25	10
Cu	63	700	75	9.3	40
Zn	66	2600	50	52	25
As	75	75	5	15	2.5
Zr	90	750	10	75	5
Ag	107	500	100	5	50
Cd	111	50	35	1.4	20
Sn	118	30	10	3	5
W	182	50	15	3.3	7.5
Hg	202	75	75	1	40
Tl	205	20	10	2	5
Pb	208	150	20	7.5	10
Bi	209	15	5	3	2.5

Table 4. Removal of Elements from a 2% Hydrochloric Acid Blank, -0.75 V Applied to Working Electrode

	m/z	Initial Signal (c/s)	Final Signal (c/s)	Removal Factor	Final Concentration (ppt)
V	51	12000	100	120	50
Cr	53	40000	100	400	50
Mn	55	1800	1000	1.8	500
Fe	57	6000	4000	1.5	2000
Co	59	50	10	5	5
Ni	60	300	40	7.5	20
Cu	63	500	120	4.2	60
Zn	66	1500	200	75	100
As	75	1200	250	4.8	125
Zr	90	250	10	25	5
Ag	107	600	150	4	75
Cd	111	75	50	1.5	25
Sn	118	250	15	16.7	7.5
W	182	50	20	2.5	10
Hg	202	300	100	3	50
Tl	205	100	10	10	5
Pb	208	2000	25	80	12.5
Bi	209	75	15	5	7.5

Table 5. Removal of Elements from a 10% Nitric Acid Blank, -0.75 V Applied to Working Electrode

	m/z	Initial Signal (c/s)	Final Signal (c/s)	Removal Factor	Final Concentration (ppt)
V	51	1800	15	120	7.5
Cr	53	700	25	28	12.5
Mn	55	2500	1000	2.5	500
Fe	57	4000	2500	1.6	1250
Co	59	85	10	8.5	5
Ni	60	250	25	10	12.5
Cu	63	14000	100	140	50
Zn	66	1150	75	15.3	37.5
As	75	15	5	3	2.5
Zr	90	250	10	50	2.5
Ag	107	1950	700	2.7	350
Cd	111	900	35	25.7	25.7
Sn	118	200	10	20	5
W	182	150	25	6	12.5
Hg	202	125	75	1.7	40
Tl	205	105	15	7	7.5
Pb	208	250000	50	5000	25
Bi	209	120	10	12	5

Table 6. Removal of Elements from a 10% Sulfuric Acid Blank, -0.75 V Applied to Working Electrode

	m/z	Initial Signal (c/s)	Final Signal (c/s)	Removal Factor	Final Concentration (ppt)
V	51	5000	20	250	10
Cr	53	220	50	4.4	25
Mn	55	3050	1500	2	750
Fe	57	3050	2250	1.4	1125
Co	59	55	5	11	2.5
Ni	60	800	50	16	25
Cu	63	2150	75	28.7	37.5
Zn	66	10000	100	100	50
As	75	150	5	30	2.5
Zr	90	350	10	35	5
Ag	107	4000	150	26.7	75
Cd	111	155	35	4.4	25.7
Sn	118	95	10	9.5	5
W	182	135	15	9	7.5
Hg	202	230	75	3.1	40
Tl	205	65	10	6.5	5
Pb	208	1150	20	57.5	10
Bi	209	80	5	16	2.5

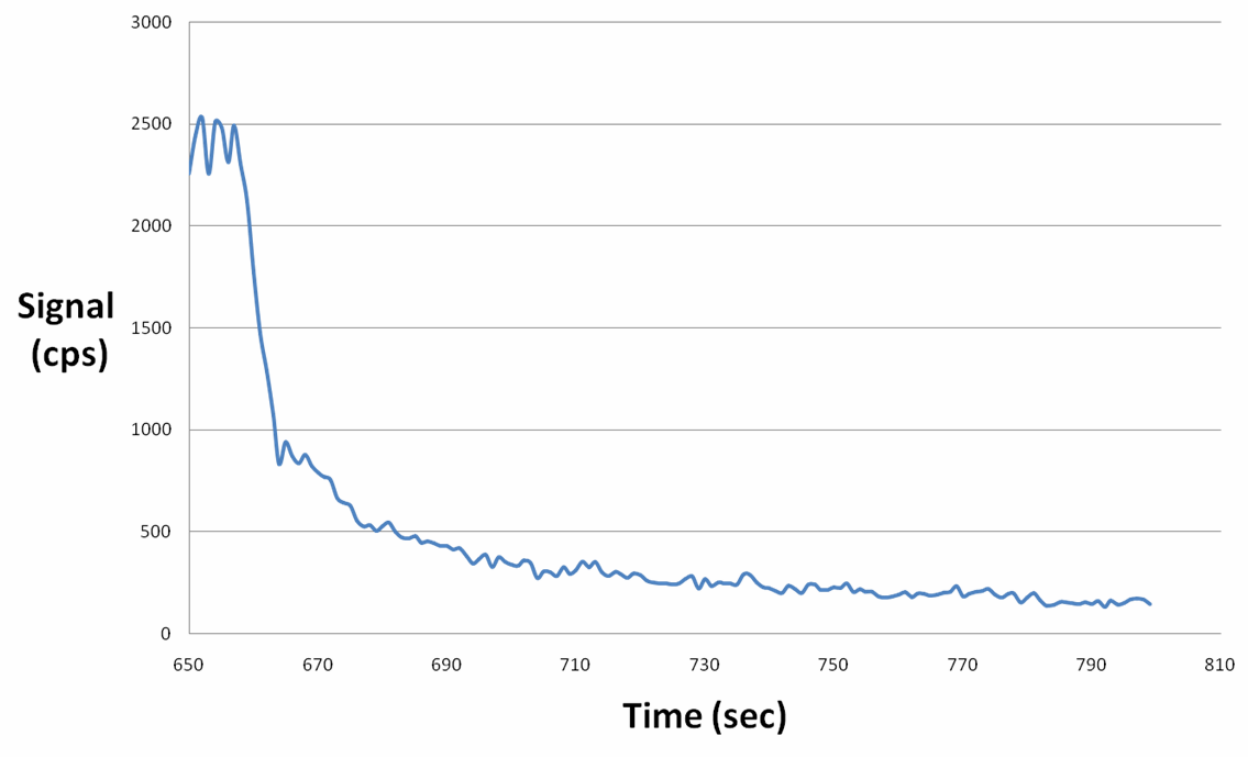

Fig. 6. Removal of As spiked at 5 ppb into 1% HNO_3, m/z = 75, -0.75 V on working electrode.

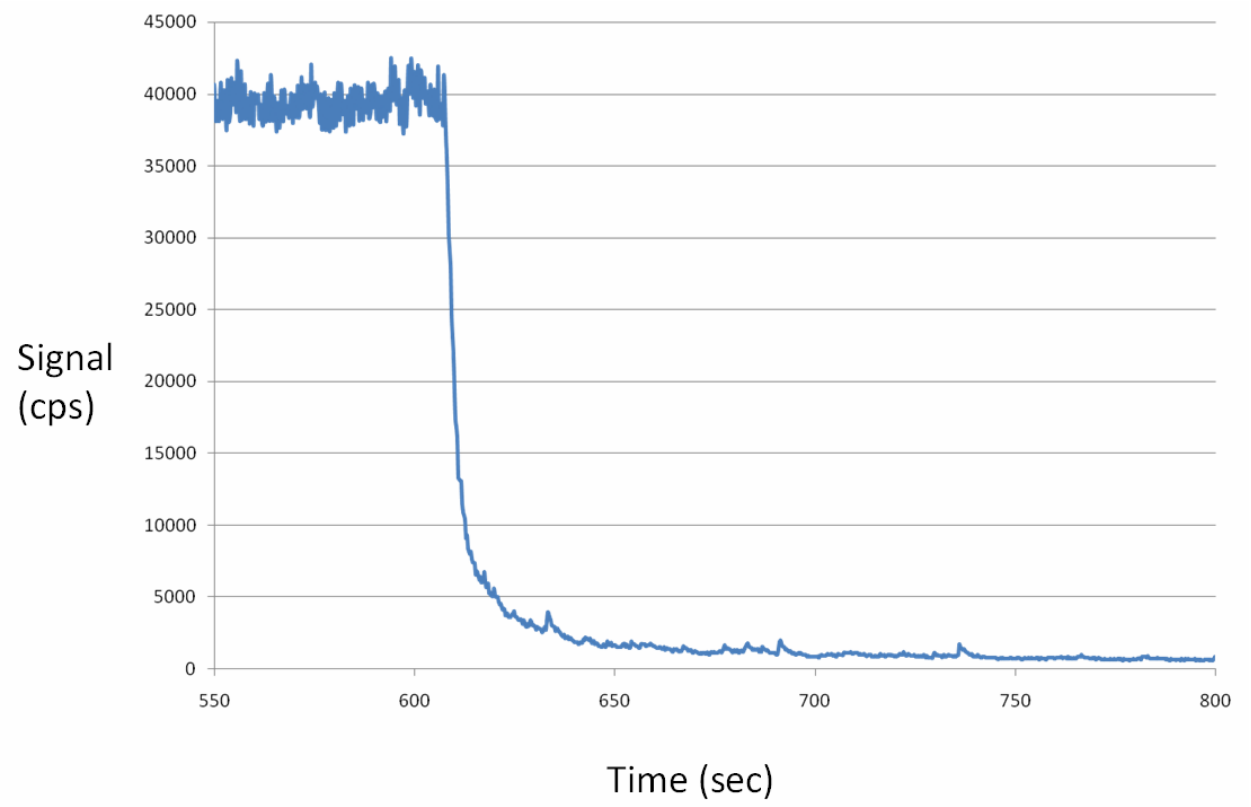

Fig. 7. Removal of Hg spiked at 10 ppb into 1% HNO_3, m/z = 202, -0.75 V on working electrode.

Chapter 3. Reduction of Matrix Effects in Inductively Coupled Plasma Mass Spectrometry by Flow Injection with an Unshielded Torch

A paper to be submitted to the *Journal of Analytical Chemistry*

Cory T. Gross and R.S. Houk

Ames Laboratory-U. S. Department of Energy, Department of Chemistry, Iowa State University, Ames, Iowa 50011 USA

Abstract

Solution samples with matrix concentrations above ~0.1% generally present difficulties for analysis by inductively coupled plasma mass spectrometry (ICP-MS) due to cone clogging and matrix effects. Flow injection (FI) is coupled to ICP-MS to reduce clogging from samples such as 1% sodium salts and seawater. Surprisingly, matrix effects are also less severe during flow injection, at least for some matrix elements on the particular instrument used. Sodium chloride at 1% Na and undiluted seawater cause only 2 to 29 % losses of signal for typical analyte elements. A heavy matrix element (Bi) at 0.1% also induces only ~14% loss of analyte signal. However, barium causes about the same matrix effect as usual. Also, matrix effects during FI are of the usual magnitude when a metal shield is inserted between the load coil and torch, which is the most common mode of operation for the particular ICP-MS device used.

Introduction

ICP-MS is a sensitive and accurate means to determine the trace element content of solutions. Unfortunately, the analyte signal depends not only on analyte concentration but also on the concentration and identity of matrix elements. Many previous studies show that matrix elements usually suppress analyte sensitivity [1-10]. Such signal losses are usually blamed mainly on space charge effects as the ions leave the skimmer [1, 11, 12]. However, signal enhancements caused by matrix elements are occasionally seen [13]. Solid materials from the sample matrix also coat onto the sampler and/or skimmer cone, which is one cause of signal drift.

Internal standardization is commonly used to correct for these problems. In general, the quality of the internal standardization correction is best if the extent of signal loss is less severe. Since the magnitude of the matrix effect varies with the atomic weight of the analyte ion [4, 14], a suite of different internal standard elements that span the m/z range are usually added to correct for matrix effects in multielement analysis.

Thus, the total solute content of the sample is usually restricted to no more than 0.1% in ICP-MS. Chemical separations for matrix removal and/or analyte preconcentration are one option for analyzing samples with higher matrix

levels [15-20], but most analysts prefer to simply analyze the sample as is. Alternative procedures that attenuate matrix effects and cone clogging could allow more routine measurements at lower dilution factors, which would have various analytical benefits. Introduction of only a discrete plug of sample solution by FI attenuates cone clogging [21, 22]. Memory effects are also reduced by FI, and sample rinse-out times are shortened.

Recent FI experiments in our lab indicate that the matrix effect can also be attenuated in this fashion, at least for one type of instrument and certain sample matrices. These observations are described in the present work.

Experimental Section

ICP-MS Instrumentation. These experiments were performed on a quadrupole ICP-MS (HP 4500, now Agilent, Santa Clara, CA). The operating parameters (Table 1) were selected in the usual fashion, to give optimal signal with tolerable levels of CeO^+ (~2%) and Ce^{2+} (~1%, relative to Ce^+) ions from clean multielement standards. The torch was not shielded (i.e., the shield was not present) in all except the last result reported below.

FI and Sample Introduction. The Babington nebulizer originally supplied with the instrument was replaced with a microconcentric nebulizer (PFA-100, Elemental Scientific Inc., Omaha ,NE, nominal uptake rate ~ 100 μL/min). The spray chamber was the standard double pass type, internal volume ~ 70 mL, cooled to 2°C.

FI was performed with an autosampler equipped with a programmable sample valve and loops (Model SC-2, Elemental Scientific Inc., Omaha, NE). This device featured an onboard vacuum pump to quickly deliver solution to the sample loop which was then injected via a computer controlled injection valve. To minimize dispersion, the loop and valve were mounted as close to the nebulizer as possible; the dead volume in the liquid between loop and nebulizer was only ~20 μL.

Sample Preparation and Standard Solutions. One set of samples was prepared by dissolving weighed amounts of solid NaCl (certified A.C.S. grade, Fisher Scientific, Fair Lawn, NJ) into a multielement standard solution (Spex Certiprep, Metuchen NJ) containing 10 ppb of various analytes, including Li, Sc, Y, Ce, and Tl. These elements were chosen to span the entire mass range. Final matrix concentrations were 1000 ppm, 2000 ppm, 5000 ppm, and 10,000 ppm Na. Matrix blanks containing only NaCl were also prepared and analyzed; none of these matrix blanks contained appreciable analyte.

The second group of solutions was prepared using a coastal seawater reference material (CASS-1, ~3% total salts, acidified to pH 1.6 with nitric acid by the supplier, Marine Analytical Chemistry Standards Program, Division of Chemistry, National Research Council of Canada (NRCC), Ottawa, ON, Canada). This sample was diluted to varying degrees: 10x, 5x, 2x, and 1x (i.e., no dilution). Each of these dilutions and the undiluted portion were also spiked with 10 ppb of the same multielement standard described in the previous paragraph. The seawater sample was spiked to minimize possible contributions from polyatomic ions in subsequent measurements of matrix effects. The unspiked seawater sample was analyzed and found to contain negligible amounts of the analyte elements except Li. Again, signals from the seawater samples were compared to those from the 10 ppb clean multielement standard. These seawater samples all contained HNO_3 at 1%.

The Ba matrix samples were prepared by dissolving weighed amounts of solid $BaCl_2$ (certified A.C.S grade, Fisher Scientific, Fair Lawn, NJ) into the same multielement standard described in the NaCl preparation. Final Ba matrix concentrations were 1000 ppm, 5000 ppm, and 10,000 ppm. Bismuth matrix samples were prepared using a 1000 ppm Bi

elemental standard (PlasmaChem, Bradley Beach, NJ). The 1000 ppm Bi and a 500 ppm dilution were spiked with 5 ppb of Li, Sc, Y, Ce, and Tl. Again, matrix blanks of the Ba and Bi matrix solutions were found to contain negligible amounts of the analyte.

All dilutions performed with distilled deionized water (18 MΩ, Nanopure-II, Barnstead Co., Newton, MA). All solutions were acidified to 1% HNO_3 (A.C.S. reagent grade plus, Fisher, Fair Lawn, NJ).

Data Acquisition. Samples were loaded into the sample rack of the autosampler, which was programmed to fill the sample loop and open the injection valve for the appropriate length of time. Injections of 1, 5, and 10 seconds were tested in FI mode. When the sample was not being injected a 100 µl/min carrier flow of 1% HNO_3 was continuously nebulized to keep solvent load on the plasma constant.

Data were collected in each injection for the five analyte elements (Li, Sc, Y, Ce, and Tl at m/z = 7, 45, 89, 140, and 205 respectively) and presented in time resolved mode. The integration period for each m/z was 0.01 s, which was fast enough to cover the FI peak for the shortest (1 s) injections tested. After the injection of a sample the sample probe was double rinsed in 1% HNO_3, and the process was repeated. The matrix effect is measured by comparing the steady state signal for each element with matrix present to that in clean standard solutions. Peak areas were used for the 1 s injections because the signals did not reach the steady state level.

Results and Discussion

Matrix Effects from NaCl. For reference, results obtained during continuous sample introduction are shown first (Figure 1a), using Tl as the analyte element. Here the FI system was removed and the sample was aspirated by natural uptake at ~ 100 μl/min, the same flow rate used subsequently. Signal is observed between ~35 and 60 s after the sample is changed. At 2000 ppm Na, Tl^+ signal is suppressed by ~32%. At 10,000 ppm Na, the suppression is worse, and clogging causes the signal to fall soon after injection. Other, lighter elements are suppressed even more extensively (Table 2). The matrix effects observed for continuous injection in Figure 1a and Table 2 are more or less the norm in ICP-MS.

Analogous results from FI experiments are described next. For the 1 s injections (Figure 1b), Na at 5000 ppm causes only ~ 15% loss of Tl^+ signal. Similar suppression curves were obtained for 1000 and 2000 ppm Na; the data are not plotted for clarity. The 10,000 ppm Na solution suppresses Tl^+ signal more extensively, but still only by ~ 30%.
Injections for 5 and 10 s (Figures 2a and 2b) are long enough to reach the steady state briefly. The suppressions observed for a given matrix concentration at these longer injections are similar to each other. Note that the actual signal levels differ among the various plots. These experiments were done over a period of several months, and factors like detector gain, cone condition, and small variations in selection of operating conditions affect the signal seen on a given day. Note also that analyte signals from the matrix blanks are negligible in Figures 1 and 2.

Matrix effects from NaCl for continuous introduction and FI (5 s injections) are summarized for the five analyte elements in Table 2. Here signal recovery is expressed as

the ratio (analyte signal from matrix solution/analyte signal from clean solution) x 100%. When the sample is introduced by FI, the matrix effects for each analyte are still present, but they are much less pronounced.

If the matrix effect is less extensive, perhaps the quality of corrections derived from internal standardization is also improved. Table 3 illustrates this to be the case; a single internal standard element (Y^+) does a much better job of correction for the FI results. In some cases, the quality of the internal standard corrections approaches the inherent limit of the measurement precision, typically no better than ~ 2%. Thus, there is less need for multiple internal standard elements with FI.

Matrix Effects in Seawater Samples. Seawater is generally diluted extensively before analysis by ICP-MS; some analyte elements require chemical matrix removal and/or preconcentration. Compared to the previous results for a synthetic NaCl matrix, similar improvements in signal recovery are seen with seawater samples during FI. Representative results are shown for Ce^+ in Figure 3. Even for undiluted seawater, the Ce^+ signal is suppressed by only ~26%. The signal recoveries for all analyte elements in seawater are summarized in Table 4.

Results for Li in seawater are not shown because the sample had substantial Li originally. Also, the nebulizer performed poorly if straight seawater was nebulized continuously, so matrix effects during continuous nebulization were not evaluated for seawater. Undiluted seawater could be injected repeatedly by FI for 10 s intervals without appreciable signal loss due to cone clogging, in general agreement with other observations that FI greatly reduces deposition on the cones [21, 22]. Of course, the sample also rinses in and out faster by FI.

Effects of Other Matrix Elements. The matrix effect is usually more extensive the greater the atomic weight of the matrix element [4, 14]. Traditionally, this variation is considered to be an attribute of space charge effects [14]. Thallium signals from Bi solutions up to 1000 ppm are shown in Figure 4a. Although the signal recovery in Bi matrix is moderately worse than with the Na matrix, it is again much better than usual.

A similar experiment with barium matrix (Figure 4b) shows a quite different result. Originally, we considered Ba to simply act as a matrix element with an intermediate atomic weight between that of Na and Bi. Thus, we expected only small matrix effects during FI. However, Figure 4b shows that the matrix effect from Ba remains substantial, more like those observed during continuous nebulization.

Why should Ba be different from the other matrix elements studied? It forms substantial numbers of M^{2+} ions, and the main ionization form (Ba^{+}) has accessible electronic states with excitation energies in the visible. The most abundant matrix elements (i.e., the Na in seawater) in the other samples studied lack these characteristics.

Matrix Effects with a Shielded Torch. Modern versions of this particular ICP-MS instrument usually use a metal shield inserted between the load coil and torch. This shield reduces capacitive coupling between the load coil and plasma, thus the plasma potential is lower with the shield [1, 23,24]. A lower plasma potential yields ions with a narrower spread of kinetic energy, which improves sensitivity and is particularly valuable when a collision cell is used to reduce polyatomic ion interferences by kinetic energy discrimination [25].

The effect of NaCl matrix on Sc signal with a grounded shield present during FI is shown in Figure 5. Here the same forward power is used as in the previous results, but the sample gas flow rate is adjusted to re-optimize Ce^{+}, CeO^{+} and Ce^{2+} signals.

First, note that the shield improves the Sc^+ signal for the clean standard by ~ 3X, in agreement with other observations. Note also that the matrix effect is more like that seen in conventional ICP-MS experiments, i.e., 40% signal loss at 1000 ppm Na, 90% signal loss at 10,000 ppm Na. Thus, whether the torch is shielded plays a key role in the extent of matrix interferences, which is not expected. One report by Appelblad et al. [26] does indicate an analogous result concerning the effect of a torch shield on matrix effects with a magnetic sector instrument; in this case, the M^+ sensitivity is much higher with the shield present.

Conclusion

These observations indicate that some samples can be analyzed with less extensive dilution, fewer internal standard elements, and/or better internal standard corrections using FI. They also raise questions about the basic mechanism(s) responsible for matrix effects. Indeed, it is hard to see why the duration of the sample injection pulse should have any influence on the matrix effect if the latter occurs mainly by space charge effects inside the vacuum system. The ions pass through the sampler, skimmer and ion lens in only a few μs [1, 27], much faster than even the shortest FI injections (1 s).

The observations that a) the matrix effect from Ba is much worse than that from the other elements tested, and b) the shield makes matrix effects worse, argue that matrix effects in ICP-MS can be more significant outside the sampler, in the ICP itself, than usually thought, at least on some instruments. Some indications along these lines have surfaced occasionally over the years [26, 28, 29]. Perhaps conditions in the ICP take a certain time to reach steady state after the matrix element is first added, and the properties of the matrix element differ more than previously thought. Obviously, this subject merits further study.

Acknowledgements

The authors thank Agilent for donating the ICP-MS instrument as well as ESI for donating the autosampling unit used in this research. Funding was provided by the Chemical and Biological Sciences Program, Office of Basic Energy Sciences, Ames Laboratory U. S. Department of Energy under Contract No. DE-AC02-07CH11358.

References

1. Niu; H.; Houk, R.S. *Spectrochim. Acta, Part B,* **1996**, 51, 779- 815

2. Olivares, J.A.; Houk, R.S. *Anal. Chem.*, **1988**, 58, 20-25

3. Crain, J.S.; Houk, R.S.; Smith, F.G. *Spectrochim. Acta, Part B*, **1989**, 44, 1355

4. Tan, S.; Horlick, J. *Anal. Atomic Spectrom.*, **1987**, 2, 745

5. Evans, E.H.; Giglio, J.J. *J. Anal. Atomic Spectrom.*, **1993**, 8, 1

6. Gregoire, D.C. *Appl. Spectosc.*, **1987**, 41, 467

7. Vandecasteele, C.; Nagels, M.; Vanhoe, H.; Dams, R. *Anal. Chim. Acta*, **1998**, 211, 91

8. Kawaguchi, H.; Tanaka, T.; Nakamura, T.; Morishita, M.; Mizuike, A. *Anal. Sci.*, **1987**, 3, 305

9. Hobbs, S.E.; Olesik, J. *Appl. Spectrosc.*, **1991**, 45, 1395

10. Lazar, A.C.; Farnsworth, P.B. *Appl. Spectrosc.*, **1999**, 53, 465-470

11. Gillson, G.R.; Douglas, D.J.; Fulford, J.E.; Halligan, K.W.; Tanner, S.D. *Anal. Chem.*, **1988**, 60, 1472

12. Tanner, S.D. *Spectrochim. Acta, Part B*, **1992**, 47, 809

13. Liu, S; Beauchemin, D. *Spectrochim. Acta, Part B,* **2006**, 61, 319-325.

14. Montaser, A., Inductively Coupled Plasma Mass Spectrometry, Wiley-VCH, NY, **1998**

15. Keil, O.; Dahmen, J.; Volmer, D. *Fresenius J. Anal. Chem.*, **1999**, 364, 694-699.

16. Alves, L.C.; Allen, L.A.; Houk, R.S. *Anal. Chem.*, **1993**, 65, 2468-2471.

17. Plantz, M.R.; Fritz, J.S.; Smith, F.G.; Houk, R.S. *Anal. Chem.*, **1989**, 61, 149-153.

18. Beauchemin, D.; McLaren, J.W.; Mykytiuk, A.P.; Berman S.S. *J. Anal. Atomic Spectrom.*, **1988**, 3, 305-308.

19. Beauchemin, D.; Berman, S.S *Anal. Chem.*, **1989**, 61 1857-1862.

20. Huang, Z.Y.; Chen, F.R.; Zhuang, X.R.; Lee, F.S.C. *Anal. Chim. Acta.*, **2004**, 508, 239-245.

21. Thompson, J.J.; Houk, R.S. *American Mineralogist*, **1982**, 67, 238-243.

22. McClenathan, D.M.; Ray, S.J.; Hieftje, G.M. *J. Anal. Aomic. Spectrom.*, **2001**, 16, 987-990.

23. Gray, A. L. *J. Anal. Atomic Spectrom.*, **1986**, *1*, 247-249.

24. Sakata, K.; Kawabata, K. *Spectrochim. Acta Part B* **1994**, *49*, 1027-1038; Sakata, K. personal communication, 1994.

25. Yamada, N.; Takahashi, J.; Sakata, K. *J. Anal. Atomic Spectrom.*, **2002**, 17, 1213-1222.

26. Appelblad, P.K.; Rodushkin, I.; Baxter, D.C. *J. Anal. Atomic Spectrom.*, **2000**, 15, 359-364.

27. Douglas, D.; French, J. B. *J. Anal. Atomic Spectrom.*, **1988**, 3, 743-747.

28. Olesik, J.; Thaxton, K.; Olesik, S. *J. Anal. Atomic Spectrom.*, **1997**, 12, 507-515.

29. Duersch, B. S.; Farnsworth, P. B. *Spectrochim. Acta Part B* **1999**, *54*, 545-555, esp. Figure 9.

Table 1. ICP-MS Operating Conditions

Forward power	1200 W
Argon gas flow rates (L/min):	
Outer	14
Auxiliary	1.5
Sample	1.05
Sampler cone	Nickel, 1.1 mm diam.
Skimmer cone	Nickel, 0.4 mm diam.
Sample depth	7.8 mm
Ion optics	
Extract 1	-227 V
Extract 2	-65 V
Einzel 1, 3	-123 V
Einzel 2	14.5 V

Table 2. Signal Recoveries (%) for NaCl Matrix

		RECOVERIES (%) AT INDICATED Na CONCENTRATIONS (ppm)					
		Continuous Flow			FI, 5 s Injections		
Analyte	m/z	1000	5000	10,000	1000	5000	10,000
Li	7	63	55	36	97	80	71
Sc	45	67	61	45	94	89	82
Y	89	69	65	57	97	91	84
Ce	140	60	50	45	87	85	80
Tl	205	68	56	38	96	91	81

Table 3. Signal Recovery Ratios (%) Using Y^+ as Internal Standard for NaCl Matrix at Indicated Na Concentrations (ppm)

		RECOVERY RATIOS (M^+/Y^+) (%) AT INDICATED Na CONCENTRATIONS (ppm)					
		Continuous Flow			FI, 5 s Injections		
Analyte	m/z	1000	5000	10,000	1000	5000	10,000
Li	7	91	85	63	100	88	84
Sc	45	97	94	79	97	98	98
Ce	140	87	77	79	90	93	95
Tl	205	98	86	67	99	100	96

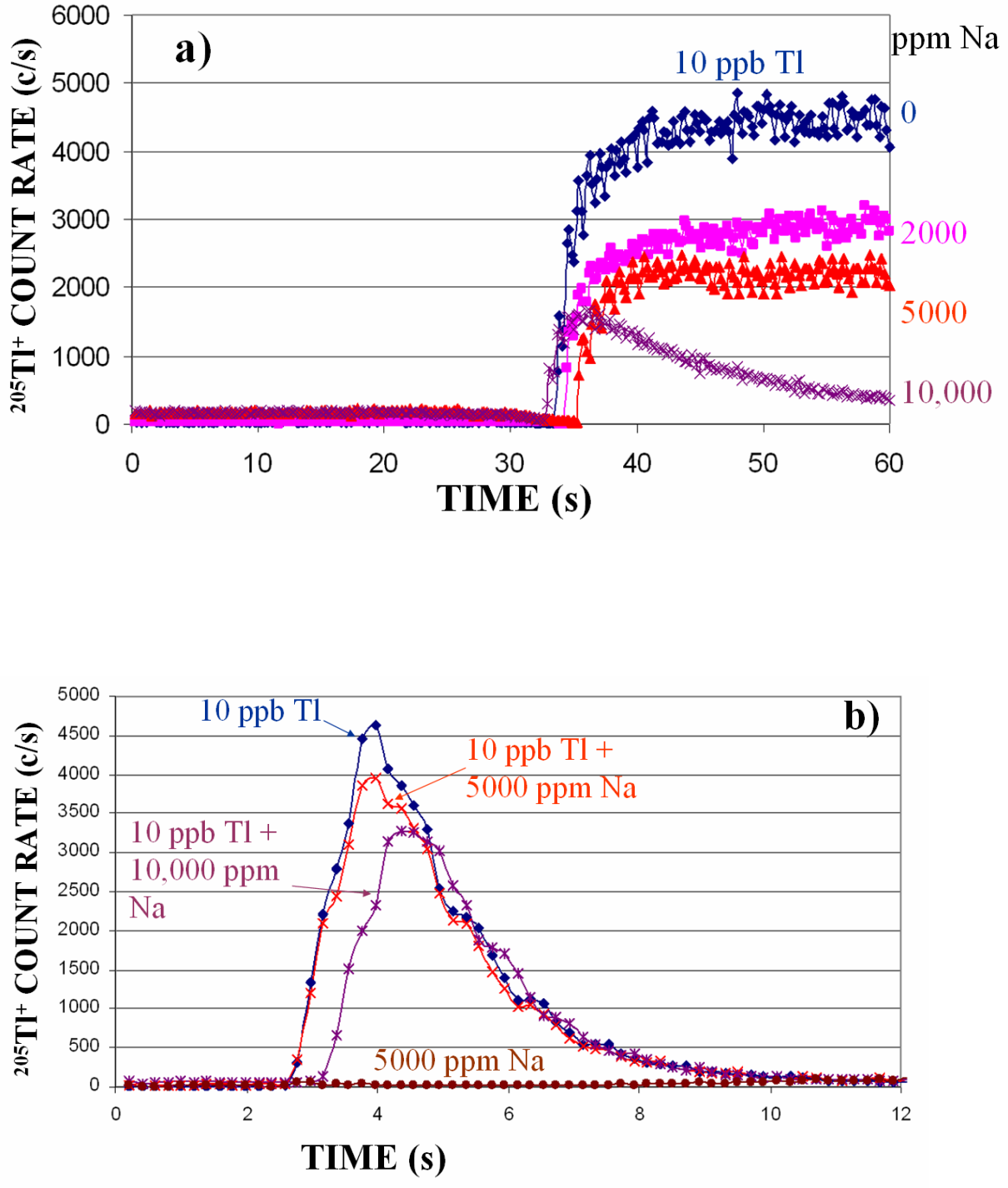

Figure 1. Matrix effects on Tl^+ signal from NaCl at indicated Na concentrations: a) continuous introduction, b) FI with 1 s injections. In b) the curves for 1000 ppm and 2000 ppm Na fall between those for Tl alone and 5000 ppm Na; these curves at intermediate Na concentrations are not plotted for clarity.

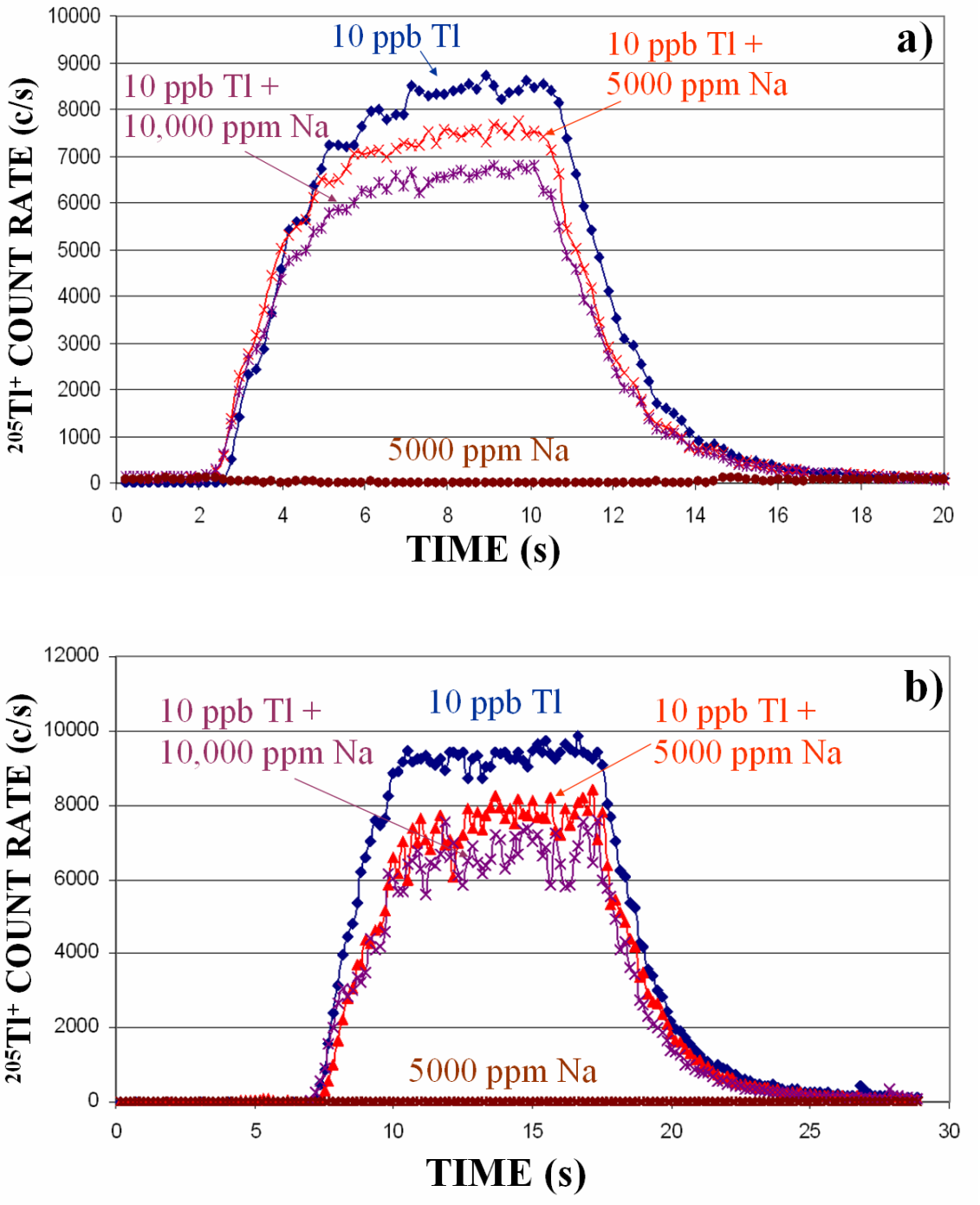

Figure 2. Matrix effects on Tl^+ signal from NaCl at indicated Na concentrations: a) FI with 5 s injection, b) FI with 10 s injections. Again, the curves for 1000 ppm and 2000 ppm Na fall between those for Tl alone and 5000 ppm Na; all the curves are not plotted for clarity. Note the different time scales in the two plots.

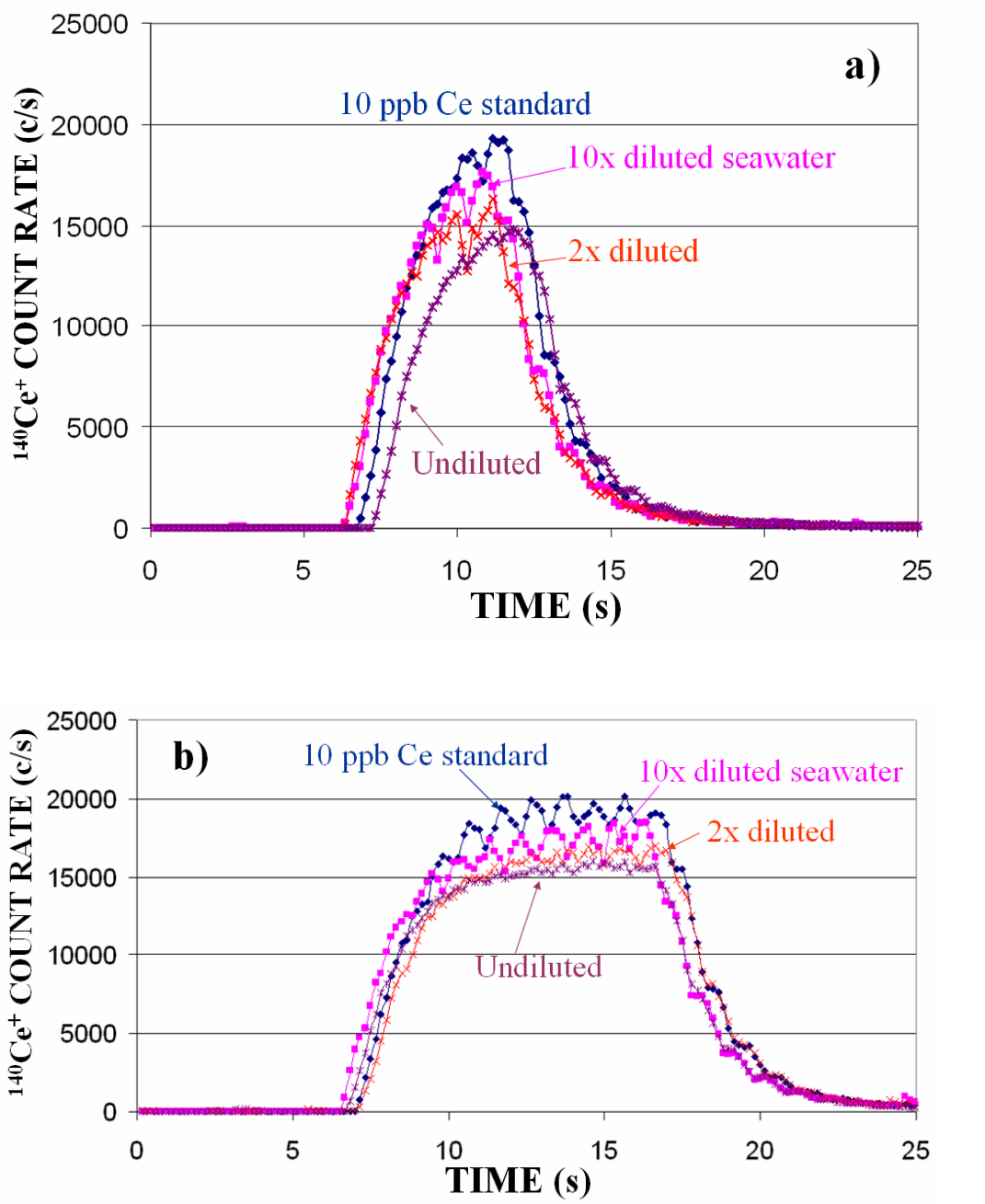

Figure 3. Matrix effects on Ce at 10 ppb in clean 1% HNO_3 standard and 10 ppb Ce spiked into CASS-1 seawater at various dilutions during FI: a) 5 s injections, b) 10 s injections.

Table 4. Signal Recoveries (%) for Seawater Matrix

		RECOVERIES (%) AT INDICATED SEAWATER DILUTIONS FI, 5 s Injections			
Analyte	m/z	10x dil.	5x dil.	2x dil.	Undil.
Sc	45	92	86	80	76
Y	89	97	95	91	86
Ce	140	90	89	85	74
Tl	205	92	86	81	76

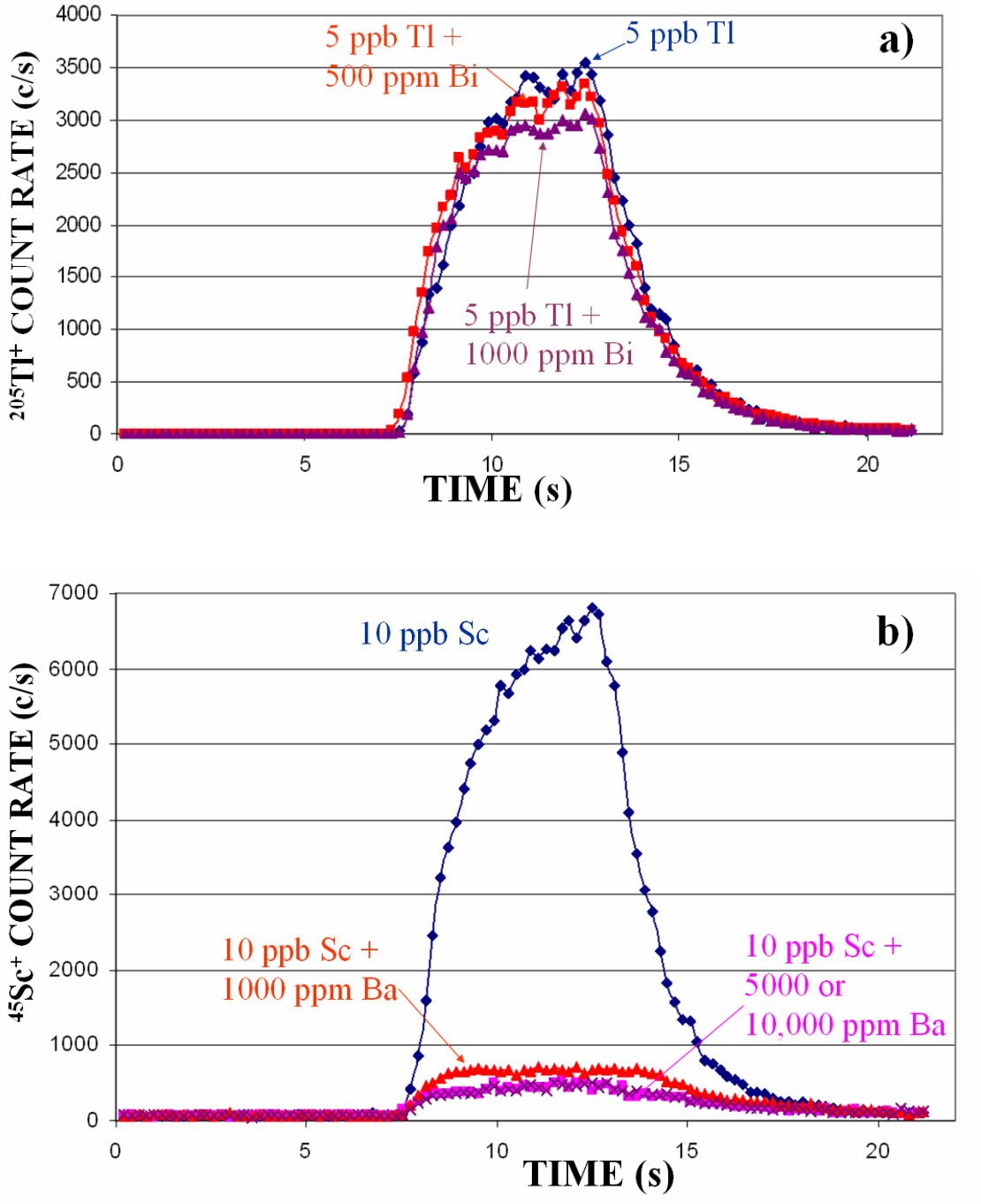

Figure 4. Matrix effects on analyte at 10 ppb, 5 s injections: a) effect of Bi matrix on Tl; b) effect of Ba matrix on Sc.

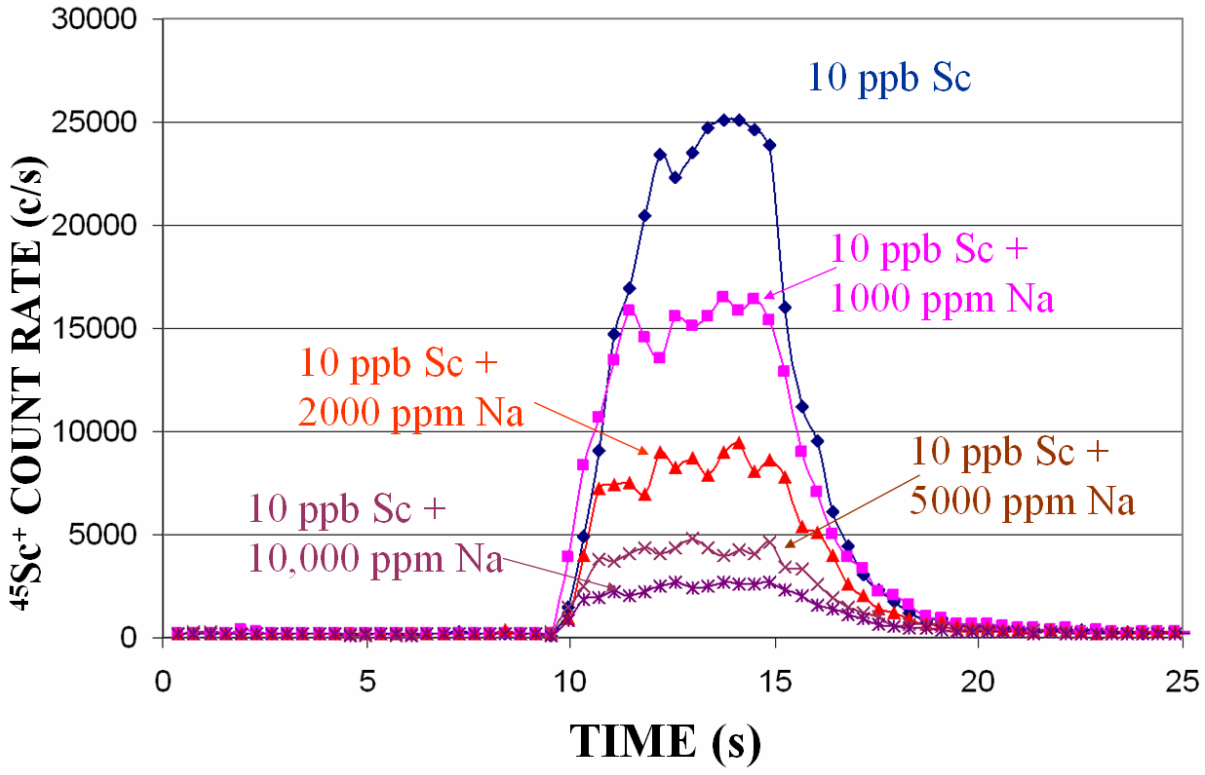

Figure 5. Matrix effects on Sc at 10 ppb, 5 s injections, for NaCl matrix at indicated Na concentrations, with grounded shield in torch.

Chapter 4. General Conclusions and Future Work

Further developments were made into uses of ICP-MS as tool for multi-elemental analysis. Specifically an instrumental add on was designed in the form of an EMLC column for use with ICP-MS. This column proved to be capable of cleaning acid blanks of many elemental contaminants. Some of the elements removed are difficult to remove by sub-boiling distillation, a popular acid cleaning method. While it can be used as a standalone option, the real value probably lies in using EMLC in conjunction with other clean sample techniques to achieve the very lowest possible blank signals. Such practices will help to keep up with the demands of fields that are requiring better and better detection limits.

Future work on this project may include testing this EMLC columns metal contaminant removal abilities on solutions other than acids, in particular organic solvents. For this application to work a supporting electrolyte would need to be added to the solvent. The time required from applying a potential to the time signal reduction is seen (~700 s) may be too long in some cases. Of course the power could be turned on at the beginning of the day and the column would then be charged and ready to use on demand. The dead volume and flow dynamics of the system could also be improved. Since the capacity of the column appears to be larger than required, at least for fairly clean blanks, miniaturization could speed up charge times and reduce dead volume.

A study of high matrix samples with fast flow injection ICP-MS yielded some surprising results. High matrix solutions analyzed by this introduction system experienced

much less severe matrix effects than expected at least on this instrumental setup. This method of analysis requires little sample prep which makes it quite advantageous to some other available techniques for running high matrix samples. Internal standards will also work better for quantification if suppression is reduced, particularly if it is possible to use a single internal standard across a large mass range which is demonstrated.

These experiments raise questions about the nature of matrix effects in ICP-MS. Why does the injection of a few seconds of sample make a difference when the timescale of the residence time in the plasma and mass spectrometer is much faster than that? Why does Ba matrix have such a severe effect? Why does having the torch shielded matter? Some of the evidence presented in these experiments suggests that the matrix effects occurring in the plasma are important too, not just what is occurring during the mass spectrometry process. These questions invite a fundamental study of the basic mechanisms of matrix effects. There are many other matrix elements and instrumental setups to test as well.

Acknowledgements

I would like to deeply thank my major professor, Dr. R.S. Houk, for years of advice, ideas, and support. His "hands off" approach to mentoring presented me with some challenges, but in the end I feel like a better scientist for it. The occasional fishing trips organized by Dr. Houk were always a welcome break from lab.

Thank you to the Houk group members I've had the pleasure of working with. Josh Messerly and Nathan Saetveit for helping me to use the Element. Everyone in the Friday Lunch Group for many a good meal.

Thanks to Dr. Marc Porter and Dan Gazda for electrochemistry knowledge that helped immensely in the early phases of the EMLC project.

Thanks to Dr. Dan Weiderin and Dave Diaz of Elemental Scientific Inc. for the use of the SC-2 auto sampler as well as the assistance in getting it setup and running.

Thank you to Dr. Basudeb Saha for letting me practically setup my own office in the Gilman instrumentation lab and for assistance whenever the HP 4500 experienced technical difficulties.

A heartfelt thanks must go out to some of the closest friends I've made in Ames. Kevin McWilliams, Amber McWilliams, Mike Vasbinder, Amie Yang, Brian Trewyn, Mike Rodriguez, Jen Nieweg, Cliff Mitchell, Mike Mitchell, Erin Rockafellow, Jin Ko, Matt

Eggers, Pat Sullivan, Josh Messerly, and Jill Ferguson who made graduate student life much more bearable.

Thanks to my dog, Lilo, for always being such a good companion. Getting a happy greeting when I get home always feels good even if things have not gone well in the lab that day. Sorry for the lack of walks while I was writing this dissertation.

Most of all I would like to thank my entire family. Especially my Mom, Dad, and brother who provide as much love and support as I could ever need.